Aspekte der Schilddrüsenphysiologie am Beispiel von Iod, TSHR und IGF-IR

Dissertation
zur Erlangung des akademischen Grades

DOCTORUM RERUM MEDICINARUM
(Dr. rer. med.)

an der Medizinischen Fakultät
der Universität Leipzig

eingereicht von: M. Sc. troph. Kathrin Haubold
geb. am 17.11.1982 in Karl-Marx-Stadt

angefertigt an der: Klinik und Poliklinik für Endokrinologie und Nephrologie
Universität Leipzig
Liebigstraße 21, 04103 Leipzig

Leiter: Prof. Dr. Michael Stumvoll

Betreuer: Prof. Dr. med., PhD, Dagmar Führer-Sakel

PD Dr. Knut Krohn

Beschluss über die Verleihung des Doktorgrades vom: 29.01.2013

Für Florian und Charlotte

iucundi acti labores

Vorbemerkung:

Für die Darstellung der Ergebnisse wurde die Form der Publikationspromotion gewählt. Die ausgewählten Publikationen enthalten die experimentellen Daten sowie die ausführliche Diskussion der jeweiligen Ergebnisse.

Verzeichnis der in der Arbeit zusammengefassten Publikationen:

Müller K*, Führer D*, Mittag J, Klöting N, Blüher M, Weiss RE, Many MC, Schmid KW, Krohn K (2011) TSH compensates thyroid specific IGF-1 receptor knockout and causes papillary thyroid hyperplasia. Mol.Endocrinol. **25:** 1867-1879.

Müller K, Krohn K, Eszlinger M, Ludgate M, Führer D (2011) Effect of iodine on early stage thyroid autonomy. Genomics **97(2):**94-100.

Inhaltsverzeichnis

1. Bibliographische Beschreibung

Müller, Kathrin, M. Sc. troph.

Aspekte der Schilddrüsenphysiologie am Beispiel von Iod, TSHR und IGF-IR

Universität Leipzig, Dissertation

53 Seiten, 70 Literaturangaben, 2 Abbildungen, 5 Anlagen (inkl. Eigenständigkeitserklärung, Curriculum Vitae, Publikationsliste)

Referat:

Die Physiologie der Schilddrüse beschreibt physikalische und biochemische Vorgänge ihrer Zellen, der Gewebe, des gesamten Organs und seiner extrinsischen Regulatoren. So vielfältig diese Vorgänge sind, gleichermaßen vielfältig sind die Einflüsse, die dieses Gleichgewicht stören können. In der hier vorliegenden Arbeit werden auf molekularer Ebene drei Regulatoren der Schilddrüsenphysiologie näher untersucht.

Der Pathologie der Schilddrüsenautonomie (SDA) liegen konstitutiv aktivierende Mutationen des TSHR zugrunde. Die Prävalenz der SDA ist in iodarmen Regionen deutlich höher. Als Ursache für Mutationen im TSHR wird vermehrter oxidativer Stress unter Iodmangel angenommen. Diese molekularen Mechanismen wurden bisher noch nicht hinreichend erforscht und führten zu der weiterführenden Fragestellung, inwiefern eine ausreichende Iodversorgung die weitere Entwicklung autonomer Thyreozyten beeinflussen kann. Mittels Microarray Untersuchungen und Funktionsanalysen eines *in vitro* Modells, konnten wir deutliche Differenzen der Genregulationen zwischen normalen und autonomen Thyreozyten durch Iod erkennen, die Auswirkungen auf Gene haben, die z.B. bei der Proliferation, dem Zellzyklus und in metabolischen Prozessen involviert sind. Wesentlich ist, dass trotz einer konstitutiven Aktivierung des TSHR Iod dennoch die Proliferation und Funktion einer frühzeitigen SDA herabsetzt.

Die physiologische Rolle des IGF-IR in der Schilddrüse *in vivo* wurde bisher nicht systematisch erforscht. Um die Rolle des IGF-IR in der Schilddrüse im Hinblick auf ihre Entwicklung und ihren normalen Metabolismus näher zu untersuchen, wurde ein Mausmodell generiert bei dem der IGF-IR schilddrüsenspezifisch über eine Cre Rekombinase (*Igf1r*TgCre) ausgeschaltet wurde. Ziel ist es nun zu untersuchen, welche Folgen ein thyreoidaler *Igf1r* Knockout auf die Funktion, Morphologie und Entwicklung der murinen Schilddrüse und deren metabolische Parameter hat. Dieser Knockout zeigt in den Mäusen keine Veränderungen des Schilddrüsengewichtes und der T_3 Serum Werte, wobei das Serum T_4 leicht absank. Allerdings waren die Serum TSH Werte bis zu 9fach erhöht. Die Histologien der *Igf1r*$^{-/-}$ Mäuse zeigten mit einer Rate von 86% papilläre Schilddrüsenhyperplasien sowie eine starke Heterogenität der Follikelstruktur. Für die molekulare Kompensation des *Igf1r* Knockouts auf Ebene der Schilddrüsenhormone in der Schilddrüse, besonders durch TSH, konnten bisher nur erste Anhaltspunkte gefunden werden.

2. Abkürzungsverzeichnis

AC	Adenylatzyklase, *adenylyl Cyclase*
ATP	Adenosyltriphosphat
BAD	BCL2 Zelltod Antagonist
BCL2	B-Zell/ Lymphom 2, *B-Cell/ Lymphoma 2*
BRAF	v-Raf mausartiges Sarkom virales Onkogen Homolog B1
cAMP	cyclisches Adenosylmonophosphat
DAG	Diacylglycerol
Epac	Austausch Protein aktiviert durch cAMP, *exchange protein activated by cAMP*
ERK 1/ 2	extrazelluläres Signal-regulatierte Kinase 1/ 2
FSH	Follikel stimulierendes Hormon
FTC	Folliculäres Schilddrüsenkarzinom, *follicular thyroid carcinoma*
GPCR	G-Protein gekoppeltes Protein, *G-Protein coupled protein*
H_2O_2	Wasserstoffperoxid
IGF-I	Insulinartiger Wachstumsfaktor I, *insulin like growth factor I*
IGF-II	Insulinartiger Wachstumsfaktor II, *insulin like growth factor II*
IGF-IR	Insulinartiger Wachstumsfaktorrezeptor, *insulin like growth factor I receptor*
IP3	Inositol-1,4,5-triphosphat
IYD	Iodotyrosin Deiodinase
LH	luteinisierendes Hormon
MAPK	Mitogenaktivierte Proteinkinase
MEK	MAPK/ERK Kinase
mRNA	Botenstoff Ribonukleinsäure, *messenger ribonucleic acid*
NIS	Natrium-Iodid Symporter
O_2	Sauerstoff
PI3K	Phosphoinositide-3-Kinase
PIP2	Phosphatidylinositol 4,5-Bisphosphat
PIP3	Phosphatidylinositol 3,4,5-Triphosphat
PKC	Protein Kinase C
PKA	Protein Kinase A
PKB/ AKT	Protein Kinase B/ V-AKT mausartiger Thymom virales Onkogen Homolog 1
PLC	Phospholipase C
PTC	papilläres Schilddrüsenkarzinom
PTEN	Phosphatase und Tensin Homolog
RAF	mausartiges Leukämie virales Onkogen Homolog 1
RAP1	GTPase-aktivierendes Protein
RAS	GTPase-artiges aktivierendes Protein
SAGE	Seriale Genexpressionanalyse
SD	Schilddrüse
T_3	Triiodthyronin
T_4	Tetraiodthyronin
TG	Thyreoglobulin
ThOX	Deiodinase, *Thyroid Oxidase*
THRSP	Schilddrüsenhormon reagierendes Protein, *thyroid hormone responsive*
TPO	Thyreodale Peroxidase
TRH	Thyreotropin freisetzendes Hormon, *thyreotropin releasing hormone*
TSH	Schilddrüsen stimulierendes Hormon, *thyroid-stimulating hormone*
TSHR	Schilddrüsen stimulierender Hormonrezeptor, *thyroid stimulating hormone receptor*

3. Einführung

3.1 Die Schilddrüsenphysiologie

Die Schilddrüse (lat. Glandula thyr(e)oidea) ist eine Hormondrüse der Wirbeltiere. Sie ist beim Menschen in zwei Lappen (Lobus dexter und sinister) unterteilt, die unterhalb des Larynx der Trachea anliegen und durch einen Isthmus miteinander verbunden sind. Bei der Schilddrüse handelt es sich um die größte rein endokrine Drüse im menschlichen Körper, die beim Erwachsenen durchschnittlich 20-30g wiegt. Die morphologische Struktur der Schilddrüse unterteilt sich in die follikulären Thyreozyten und die parafollikulären C-Zellen. Die C-Zellen sind für die Produktion von Calcitonin verantwortlich. Die Thyreozyten sind in Follikel organisiert und stellen die funktionelle Einheit der Schilddrüsenhormonproduktion dar. Diese Follikel sind in das vaskuläre Stroma eingebettet und bestehen aus einschichtig angeordneten meist kubisch bis säulenförmigen follikulären Zellen die ein zentrales Lumen umhüllen.

Gesteuert vom hypothalamisch - hypophysären Regelkreis, produzieren die Thyreozyten das Prohormon T_4 (Tetraiodthyronin) und das biologisch aktive Hormon T_3 (Triiodthyronin). Gekoppelt an das Glykoprotein Thyreoglobulin werden sie im Kolloid der Follikel gespeichert. Für die Synthese der Schilddrüsenhormone ist das Spurenelement Iod essentiell. Dabei nimmt der Na+/I- Symporter aktiv Iodid aus dem Blut in die Thyreozyten auf (Iodinierung) (1;2). Die Schilddrüsen-Peroxidase (TPO) katalysiert die Oxidation des Iodids zu Iod, unter Verwendung von Wasserstoffperoxid, und den Einbau in Tyrosin-Reste des Thyreoglobulin an der apikalen Zellmembran (3;4). Durch Exozytose werden die beiden ans Thyreoglobulin gebundenen Hormonvorläufer Monoiodthyrosin und Diiodthyrosin ins Follikellumen abgegeben. Aus zwei Molekülen Diiodthyrosin entsteht das (zu diesem Zeitpunkt noch immer ans Thyreoglobulin gebundene) Schilddrüsenhormon T_4. T_3 wird durch Koppelung von Monoiodthyrosin und Diiodthyrosin, oder auch durch Deiodinierung von T_4 in T_3 gebildet. So entsteht auch das biologisch inaktive reverse-T_3. Die abhängig vom Iodangebot unterschiedlich iodierten Thyreoglobulinmoleküle werden im Follikel gespeichert. Auch die Ausschüttung von T_3 und T_4 wird vom TSH stimuliert (5;6): Das

Thyreoglobulin des Kolloids wird durch Endozytose wieder in die Thyreozyten aufgenommen und enzymatisch zerlegt, wodurch die Schilddrüsenhormone frei werden und anschließend ins Blut abgegeben werden. (Abb. 1)

Hypothalamisch-hypophysärer Regelkreis

Das im Hypothalamus ausgeschüttete TRH (Thyreotropin Releasing Hormon) regt die Hypophyse zu einer verstärkten Ausschüttung von TSH an, was wiederum zu einer gesteigerten Bildung von T_3 und T_4 führt. In Hypothalamus und Hypophyse wird die jeweilige Bildung von TRH und TSH durch freie Schilddrüsenhormone im Blut gehemmt (Abb. 1).

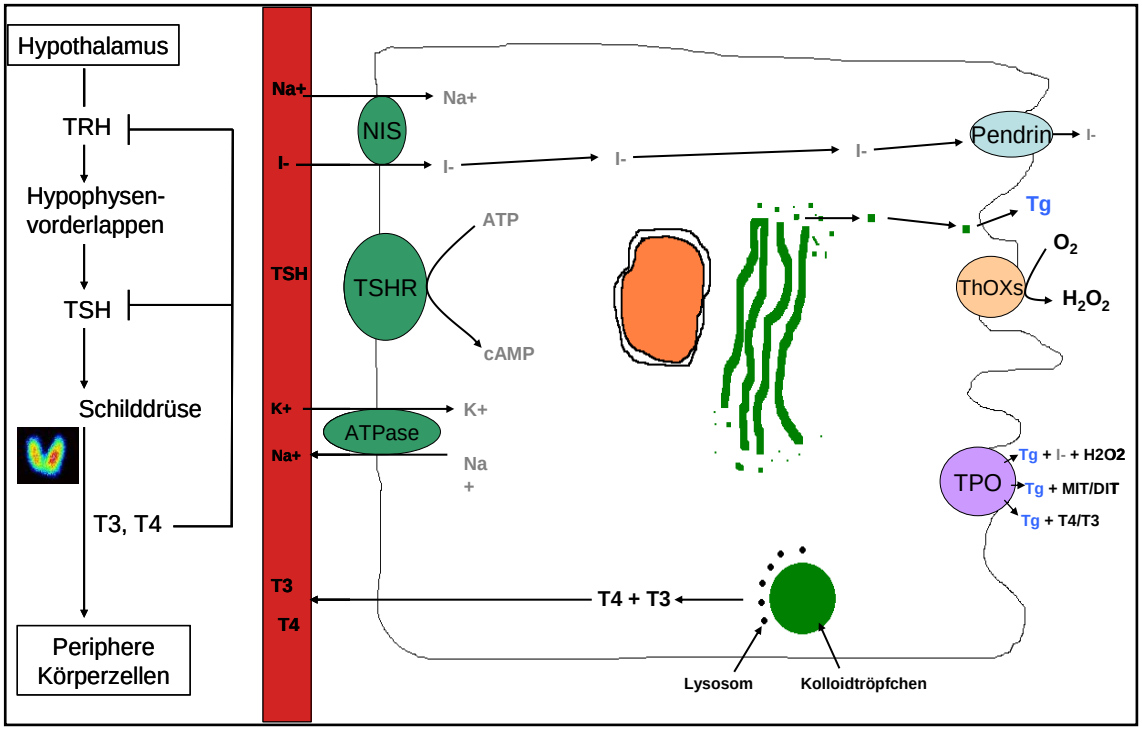

Abbildung 1: Schilddrüsenhormonsynthese gesteuert über den Hypothalamisch-Hypophysären Regelkreis. Über das basolaterale Zellmembranprotein der Follikelzellen der Schilddrüse, dem Natrium-Iodid-Symporter, wird Iod aktiv in der Schilddrüsenzelle akkumuliert. Dieser entscheidende Schritt wird durch die Bindung von TSH an den TSHR stimuliert. Die Thyroperoxidase (TPO) katalysiert unter Verbrauch von H_2O_2 die Entstehung von Iod. H_2O_2 wird durch die Schilddrüsenoxidasen 1/ 2 (ThOX 1/ 2) generiert. Iod wird schrittweise an die Tyrosylreste des Thyroglobulins gebunden. Die iodierten Tyrosylreste reagieren miteinander, so daß, Triiodthyronin (T_3, aktives Hormon) und Tetraiodthyronin oder Thyroxin (T_4, Prohormon) entstehen, die vorerst an Thyroglobulin gebunden bleiben. Das iodierte Thyroglobulin wird im Follikellumen gespeichert. Durch TSH-Stimulation erfolgt die Wiederaufnahme des Thyroglobulins durch Endozytose in die Schilddrüsenzelle. In den Lysosomen erfolgt die Degradierung des Thyroglobulins. Dabei werden T_3 und T_4 freigesetzt und in den Blutstrom abgegeben.

3.2 Rezeptorphysiologie der Schilddrüse

3.2.1 Der TSH Rezeptor

Die TSH-Rezeptor (TSHR) Signalkaskade ist der wichtigste physiologische Regulator des Schilddrüsenwachstums und der Schilddrüsenfunktion. Die Diskriminierung zwischen den unterschiedlichen TSHR- vermittelten Prozessen der downstream Signalisierung in der Zelle wie z.B. Zellwachstum oder Schilddrüsenhormonsynthese erfolgt überwiegend durch unterschiedliche Wechselwirkungen zwischen dem membranständigen Rezeptor und den intrazellulären G-Proteinen. Neben dem LH (lutropin/choriogonadotropin) Rezeptor und dem FSH (follitropin) Rezeptor gehört der TSHR (thyrotropin) zu den Glycoprotein-Hormon-Rezeptoren, einer Unterfamilie der Familie A der G-Protein-gekoppelten Rezeptoren (GPCR). Der TSHR befindet sich auf der apikalen Membran der Schilddrüsenfollikel. Die Familie A ist die größte der 3 Hauptfamilien der GPCRs. Weitere Vertreter der Familie A sind der Rhodopsin-, der Angiotensin-, der Adenosin-, der Serotonin- und der Adrenerge Rezeptor. Zur Familie B der GPCRs zählen u.a. der Secretin-, der Glucagon-, der Calcitonin- und der Parathyroid Hormon Rezeptor. Die Familie C umfasst die metabotropen Glutamat Rezeptoren, den GABAβ Rezeptoren und den Calciumsensitiven Rezeptoren. (7-9)

Der humane TSHR setzt sich aus 764 Aminosäuren zusammen und unterteilt sich in einen großen extrazellulären Abschnitt mit ungefähr 400 Aminosäuren, der als TSH Bindungsstelle dient, einen Abschnitt mit 7 transmembranen-Loops (jeweils ca. 20-27 Aminosäuren) und einem kurzen intrazellulären Abschnitt (10-12). Die Signalweiterleitung erfolgt durch Interaktion zwischen den funktionellen extrazellulären und den transmembranen Abschnitten und resultiert in der Kopplung von vier bekannten membranständigen G-Protein Familien: Gs α, Gq/11, Gi/0 and G12/13 (13-15). In der humanen Schilddrüse führt die Stimulation des TSHR zu einer Aktivierung der Adenylatzyklase und Interaktion mit G_s, wodurch cAMP zytosolisch akkumuliert wird. Ein zweiter Signalweg des TSH Rezeptors aktiviert die Phospholipase C in Wechselwirkung mit $G_{q/11}$, wodurch die sekundären Botenstoffe Diacylglycerol und Inositol-1,4,5-triphosphat zytosolisch akkumuliert werden. (14) Im

Vergleich zum Gs Signal ist eine 10fach höhere TSH Konzentration notwendig um den Phospholipase C Weg zu stimulieren (16;17). Über die cAMP Signalkaskade wird Differenzierung, Funktion und Wachstum der Schilddrüsenfollikelzellen gesteuert, wohingegen der Phospholipase C Weg die Schilddrüsenhormonsynthese und den Iodstoffwechsel der Schilddrüse kontrolliert (18;19). (Abb. 2)

3.2.3 Der IGF-IR in der Schilddrüse

Die Aktivität der Schilddrüse im Sinne ihrer Funktion und dem Wachstum sind hauptsächlich durch das hypophysäre Hormon TSH beeinflusst. Eine weitere, nicht unbedeutende Signalkaskade, läuft über den IGF-1 Rezeptor und ist Teil der reziproken Wechselwirkung mit TSH (20-22). Die Aktivierung des IGF-I Rezeptors erfolgt durch IGF-I, IGF-II oder hohen Konzentrationen an Insulin (23) (Abb. 2). Dabei wird das Zellwachstum durch die Aktivierung des B-RAF Onkogen (rat sarcoma/rat fibrosarcoma/proto-oncogene; BRAF) der MAPK Kaskade und dem Phosphatidylinositol 3-Kinase (PI3K)/AKT Weg stimuliert (1;24). Der Typ II IGFR nimmt in der Schilddrüse keinen hohen Stellenwert ein und es konnte gezeigt werden, dass vorwiegend der IGF-IR exprimiert wird (25).

Der IGF-I Rezeptor ist ein Transmembranrezeptor und zählt zu den Tyrosinkinase Rezeptoren. Strukturell baut sich der IGF-IR aus einem einzelnen Vorläuferprotein mit 1367 Aminosäuren auf und unterteilt sich in 2 alpha und 2 beta Untereinheiten, die durch Disulfidbrücken miteinander verbunden sind. Die alpha Untereinheiten liegen vollständig extrazellulär. Die beta Untereinheiten besitzen hingegen eine kurze extrazelluläre, eine hydrophobe transmembrane Region und eine Tyrosin Kinase Domaine im Zytosol. Über die Rückmeldung der Ligandenbindung an die alpha Untereinheiten, erfolgt die Tyrosin Autophosphorylierung der beta Untereinheiten und löst eine intrazelluläre Signalkaskade aus, die u.a. das Zellwachstum und Proliferation anregt. (23;26;27)

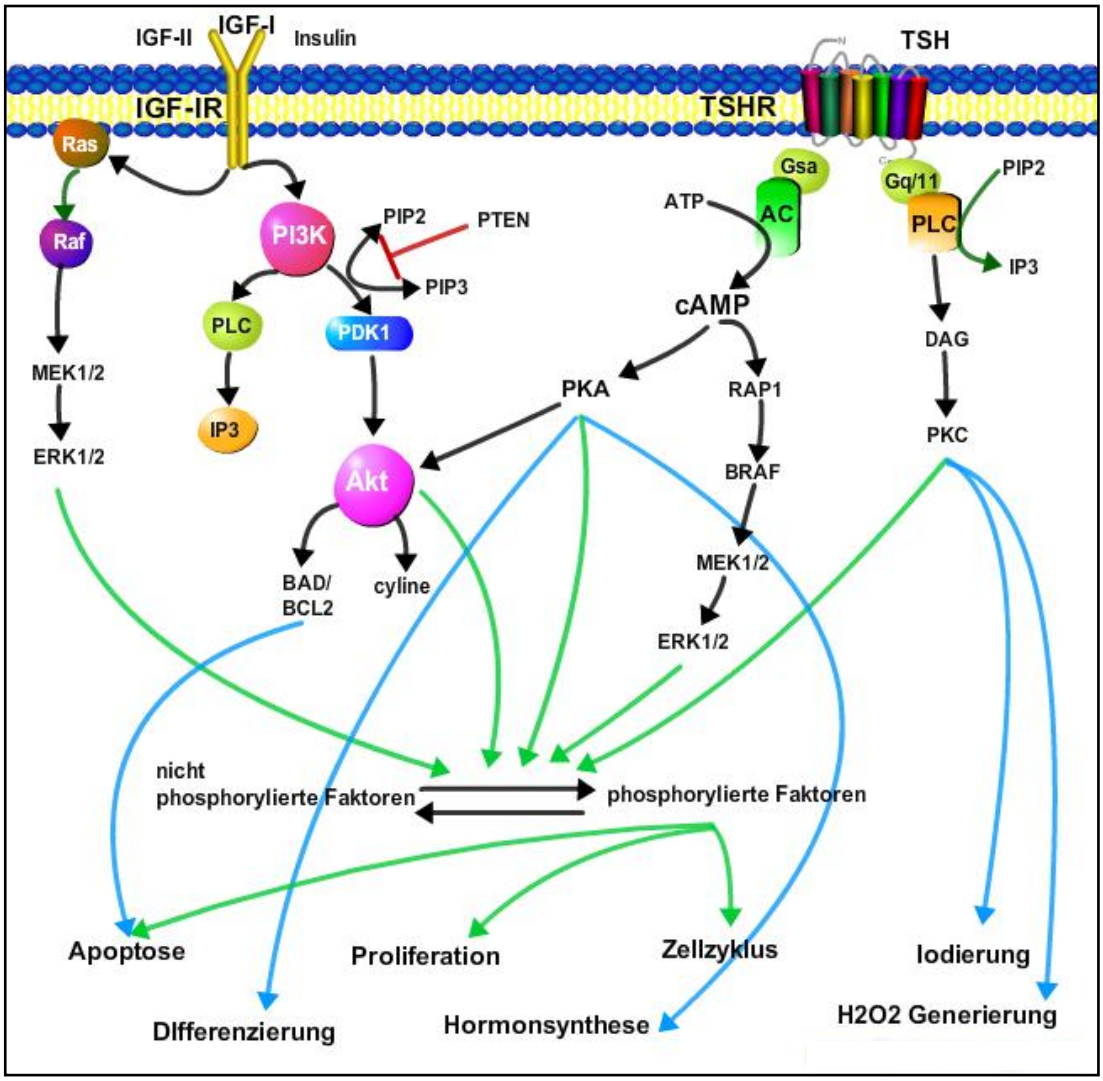

Abbildung 2: Interaktion der thyreodalen IGF-IR und TSHR Signalkaskaden. Durch Bindung der Liganden IGF-I, IGF-II und Insulin an den IGF-IR erfolgt eine Autophosphorylierung und die Stimulation des Phosphatidylinositol 3-Kinase (PI3K)/ Akt Signalweges, wodurch das Zellwachstum, Apoptose und Zellzyklus gelenkt wird. Ein weiteres IGF-IR reguliertes Signal verläuft über die Ras/ Raf Stimulation und Aktivierung der MAP Kinase/ Extracellular signal-regulated kinase 1/ 2 kurz MEK. Die für die Funktion, Wachstum und Hormonsynthese wohl wichtigste Signalkaskade der Schilddrüse, wird durch die Bindung des TSH an den TSHR aktiviert. Die vorwiegende Signalweiterleitung erfolgt über die Kopplung an die Gsα Untereinheit und führt zur Aktivierung des intrazellulären Adenylat-Cyclase (AC) - cAMP-Signalweges, wodurch die Proteinkinase A (PKA) aktiviert wird. Über diese Signaltransduktionskaskade wird sowohl die Funktion als auch die Proliferation der Schilddrüsenepithelzellen kontrolliert. Des Weiteren kann das cAMP Signal über Rap1 und BRAF die MEK Kaskade aktivieren. Die Aktivierung des Gq/11-Proteins bei höheren TSH-Konzentrationen führt über die Stimulation der Phospholipase C zur Bildung von Inositol-1,4,5-trisphosphat (IP3) und Diacylglycerol (DAG). Nachfolgend wird die Proteinkinase C (PKC) aktiviert und es erfolgt ein Anstieg der zytoplasmatischen Calciumkonzentration, welche für die Iodaufnahme und H_2O_2 Generierung verantwortlich zu sein scheint.(16;17;19) Die physiologische Bedeutung der Kopplung an Gi und G12/13 (γ) ist bisher noch nicht hinreichend geklärt. Diese Abbildung ist modifiziert dargestellt nach (28-30).

3.4 Pathogenetische Veränderungen der Schilddrüse

In Deutschland lassen sich bei ca. 20-30% der Erwachsenen noduläre Veränderungen der Schilddrüse diagnostizieren und stellen damit eine der häufigsten benignen und malignen endokrinen Erkrankungen dar.
Zu den benignen Veränderungen der SD zählen Kolloidknoten, follikuläre Adenome, Zysten, Hashimoto-Thyreoditis und die De-Quervain-Thyreoditis. Zu den malignen Veränderungen der Schilddrüse gehören u.a. Karzinome mit Follikelzelldifferenzierung (papilläres, follikuläres, gering differziertes und anaplastisches Karzinom), Karzinome mit C-Zell-Differenzierung (Medulläres SD-Karzinom, gemischtes C-Zell-Follikel-Karzinom), Lymphome, Metastasen und andere primäre Schilddrüsenkarzinome.
Zu den Schilddrüsenpathologien nicht nodulären Ursprungs zählt z.B. der Morbus Basedow (Graves Disease).
Im weiteren Verlauf dieser Arbeit werden lediglich die für diese Arbeit relevanten Schilddrüsenpathologien vertieft.

3.4.1 IGF-IR in der Schilddrüsenpathogenese

In vitro Untersuchungen konnten zeigen, dass ohne IGF-I oder hohe Konzentrationen an Insulin im Medium, TSH alleine nicht zu follikulärem Wachstum führt (22;31). IGF-I wird von Follikelzellen gebildet und weist eine höhere mRNA Expression in wachsenden im Vergleich zu nicht wachsenden Schilddrüsen und follikulären Karzinomen auf (22). Es wird daher angenommen, dass eine Kooperation zwischen der TSH Rezeptor Kaskade und dem IGF-I Rezeptor Signalweg einen entscheidenden Stellenwert in der Pathologie von follikulären Tumoren und gesundem follikulärem Wachstum einnimmt (32).
Differenzierte papilläre Schilddrüsenkarzinome zeigen eine Überexpression des IGF-I Rezeptors, die in kaum differenzierten oder undifferenzierten Karzinomen nicht zu finden ist (32). Eine Überexpression des IGF-IR in Kombination mit IGF-I führt in der Schilddrüse zu erhöhtem Drüsengewicht und vergrößertem Follikellumen, sowie erniedrigten TSH und erhöhten T_4

Spiegeln im Serum (33). Eine populationsbezogene Studie zeigt, dass erhöhtes Serum IGF-I die Bedingungen für eine Entwicklung von Struma erhöht (34). Ein Hauptregulator in der Schilddrüsenkarzinogenese ist die IGF-I Achse (32;35).

In follikulären Schilddrüsenkarzinomen (FTC) zeigt sich häufig eine Deregulation des PI3K Signalweges, welcher dem IGF-IR Signal nachgelagert ist. Der Rapamycin Signalweg tangiert in seinem Fluss den PI3K/ Akt Weg und kontrolliert essentielle Prozesse, wie Proliferation und Apoptose. Er hat sich als entscheidende Signalkaskade in der Entwicklung von FTCs herausgestellt (36). Nicht nur FTCs sondern auch papilläre Schilddrüsenkarzinome (PTC) sind charakterisiert durch eine Deregulation des MAP Kinase Signalweges oder Mutationen im *PI3K* Gen (29;37).

Eine Kategorie der papillären Schilddrüsenkarzinome, zeigt IGF-IR reiche follikuläre Zellen die arm an IGF-I mRNA Expression sind und infiltrierte benachbarte Lymphozyten die reich an IGF-I mRNA Expression und arm an IGF-I Rezeptoren sind. Dabei wird angenommen, dass die Tumorzellen ein Antigen produzieren, welches die Lymphozyteninfiltration stimuliert, und im Gegenzug die Lymphozyten IGF-I produzieren und damit das Schilddrüsenwachstum anregen (38).

Das Ausschalten des IGF-IR Signals über einen konventionellen IGF-IR Knockout in der Keimbahn führte zu zahlreichen murinen Phänotypen. Mäuse mit einer kompletten Keimbahninaktivierung des *Igf1r* Gens, sterben kurz nach der Geburt (39). Des Weiteren führt ein heterozygoter *Igf1r* Knockout in Mäusen zu einer verlängerten Lebensspanne durch eine verstärkte Resistenz gegenüber oxidativem Stress (40). Diese Daten deuten auf eine essentielle Bedeutung des IGF-IR Signalweges auf die Lebensspanne. Das vollständige Fehlen des *Igf1r* oder von Angehörigen der *Igf* Familie führt zu erniedrigtem Körpergewicht (41), Retardierung des Gehirnwachstums (42), Muskelhypoplasie (43) und zu Langlebigkeit (40) in Mäusen. Um die Relevanz des IGF-IR Signalweges in einzelnen Geweben zu erforschen, wurden transgene Mäuse mit gewebsspezifischen *Igf1r* Knockout generiert. Die gewebsspezifischen *Igf1r* Knockouts führten zu zahlreichen Störungen in den jeweiligen Organen und zu sekundären Effekten im Organismus (44-48). Gewebsspezischer *Igf1r* Genknockout in weißem Fettgewebe führt zu

erhöhten IGF-I Konzentrationen im Serum, erhöhten *Igf1* mRNA Level der Leber und des Fettgewebes kombiniert mit erhöhtem Lebergewicht (49).

3.4.2 Mutationen des TSHR

Der TSHR nimmt für die Schilddrüse eine besondere Stellung ein, weil er sowohl Ziel für Autoantikörper ist als auch ein breites Spektrum an Mutationen zeigt, die entweder seine Signale aktivieren („gain of function“ Mutationen) oder seine Funktionalität einschränken („loss of function“ Mutationen) (30;50). Es wird im Ursprung zwischen somatischen, sporadischen und Keimbahnmutationen unterschieden.

Somatische, konstitutiv aktivierende *TSHR* Genmutationen zeigen sich in vielen benignen Schilddrüsentumoren. Sie werden als heiße Knoten oder Adenome diagnostiziert und verursachen im Spätstadium eine Hyperthyreose. Allerdings werden somatische Mutationen des TSHR auch in malignen Tumoren (Schilddrüsenkarzinom) gefunden und resultieren in konstitutiver Aktivierung des TSH Rezeptors. Diese „gain of function“ Mutationen zeigen sich auch bei Keimbahnmutationen im *TSHR* und liegen meist in einem der 7 transmembranen Abschnitte des TSHR (51). Im Gegensatz dazu können Hypothyreose und Schilddrüsenhyperplasie bei einer Inaktivierung des cAMP Signalweges auftreten, die durch nichtfunktionelle TSHR Mutationen verursacht wird (30;52).

Beispiele für „gain of function“ Mutationen im TSHR Gen sind Aminosäuremaustausche an Position 453, 629 und 623. Beispiele für „loss of function“ Mutationen im TSHR Gen sind Aminosäuremaustausche an Position 162, 525, und 620. Des Weiteren werden auch Deletionen beschrieben, die zu einer funktionellen Aktivierung bzw. Inaktivierung des TSH Rezeptors führen können. Die Universität Leipzig betreibt eine Datenbank für TSHR Mutationen, in der bereits beschriebene TSHR Mutationen aufgelistet sind (http://endokrinologie.uniklinikum-leipzig.de/tsh/) (53).

3.4.3 Schilddrüsenautonomie

Die Schilddrüsenautonomie definiert sich als eine TSH unabhängig gesteuerte Funktion und Proliferation der follikulären Schilddrüsenzellen (19;54). Sie klassifiziert sich in unifokale, multifokale und disseminierte Schilddrüsenautonomien. Als Hauptursache für das Auftreten einer Autonomie der Schilddrüse werden Mutationen am TSHR verantwortlich gemacht, die zu einer konstitutiven Aktivierung der cAMP Signalkaskade führen und so die Funktion und das Wachstum der Schilddrüse steigern (30;55;56). Konstitutiv aktivierende Mutationen des TSHR sind u.a. L629F und A623I.

Die höchste Prävalenz der SD-Autonomie zeigt sich in Iodmangelgebieten und selten in Gebieten mit ausreichender Iodversorgung (57;58). Eine humane Studie aus Pescopagano konnte zeigen, dass Iodmangel ein Selektionsfaktor für die Entstehung einer klinisch relevanten SD-Autonomie ist (59). Der molekulare Zusammenhang zwischen der Entstehung einer SD-Autonomie und Iodmangel ist noch nicht vollständig geklärt. Ursächliche Hinweise liefern *in vivo* Daten von Mäusen und Ratten bei denen gezeigt werden konnte, dass in einer Iodmangel Situationen die mRNA Expression von oxidativen Abwehrgenen in der SD erhöht sind (60). Diese Hypothese basiert auf der Annahme, dass unter Iodmangel vermehrt reaktive Sauerstoffspezies (ROS) entstehen, da H_2O_2 als Cosubstrat der Thyroglobulin Iodierung vermehr gebildet aber nicht hinreichend umgesetzt wird.

Die Auswirkungen von Iod auf die kontinuierliche Entwicklung einer klonalen Schilddrüsenautonomie in Bezug auf klinisch relevante Schilddrüsenerkrankungen, wurde auf der molekularen Ebene noch nicht untersucht. Iod spielt eine entscheidende Rolle in der Regulation des Schilddrüsenwachstums und deren Funktion. Supraphysiologische Ioddosen sind dafür bekannt die Schilddrüsenhormonsynthese zeitlich zu inhibieren. Dieser Prozess wird nach seinem Entdecker Wolff-Chaikoff benannt und in der präoperativen Phase als „Plummering“ bei einigen Patienten genutzt, die sich in einer thyreotoxischen Krise befinden. Ferner konnte gezeigt werden, dass ein Iodüberschuss zu einer Inhibierung des Zellwachstums, einer Induktion der Apoptose und zu Veränderungen der Zellmorphologie führt (61).

Rein hypothetisch müsste dann eine vermehrte Iodaufnahme die Proliferation von autonomen Thyreozyten dämpfen und somit die Ausprägung des autonomen Wachstums verlangsamen und möglicherweise eine Hyperthyreose verhindern.

4. Ziel der Arbeit

Ziel dieser Arbeit ist die Untersuchung molekularer Regulationsmechanismen der Schilddrüsenphysiologie (TSHR, Iod und IGF-IR). Dabei wurde der Fokus auf zwei zentrale Aspekte der Rezeptorphysiologie in der Schilddrüse, TSHR und IGF-IR, gelegt.

1. Der Einfluss einer ausreichenden Iodversorgung auf die Entwicklung/ Ausprägung einer frühzeitigen Schilddrüsenautonomie. I*n vivo* Studien zeigen einen Zusammenhang zwischen Iodmangel und erhöhter mRNA Expressionen von oxidativen Abwehrgenen (60), der auf einer vermehrten Bildung von oxidativen Sauerstoffspezies beruhen könnte (62).
Um zu untersuchen, ob Iod einen inhibitorischen Effekt auf die Ausprägung einer Schilddrüsenautonomie haben könnte, wurde ein *in vitro* Model der klonalen Schilddrüsenautonomie (55) mit Iod inkubiert. Dabei erfolgten Genexpressionstudien sowie die Analyse von Funktion und Proliferation der Thyreozyten mit und ohne Iodsupplementation.

2. Trotz seiner Bedeutung für die Schilddrüsenphysiologie, ist der IGF-I Signalweg in der Schilddrüse noch nicht hinreichend erforscht. Es liegen bereits Studien vor in denen der *Igf1r* ubiquitär und gewebsspezifisch ausgeknockt wurde und die Hinweise auf dessen Relevanz bezüglich Wachstum, Lebensspanne, IGF-I Serumspiegel, Körpergewicht und Gehirnretardierung liefern (39-42;49). Um die Rolle des IGF-IR in der Schilddrüse bezüglich deren Entwicklung und Metabolismus näher zu untersuchen, wurde als weiterer Teil der Promotionsarbeit ein Mausmodell generiert bei dem der IGF-IR schilddrüsenspezifisch über eine Cre Rekombinase (*Igf1r*^{TgCre}) ausgeschaltet wurde. Ziel ist es nun zu untersuchen, welche Folgen ein thyreodaler *Igf1r* Knockout auf die Funktion, Morphologie und Entwicklung der murinen Schilddrüse und ihrer metabolischer Parameter hat.

5. Publikationen

5.1 Effect of iodine on early stage thyroid autonomy

Genomics 97 (2011) 94–100

Contents lists available at ScienceDirect

Genomics

journal homepage: www.elsevier.com/locate/ygeno

Effect of iodine on early stage thyroid autonomy

Kathrin Müller [a], Knut Krohn [b], Markus Eszlinger [a], Marian Ludgate [c], Dagmar Führer [a,*]

[a] Department of Internal Medicine, Division of Endocrinology and Nephrology, University of Leipzig, Leipzig, Germany
[b] Interdisciplinary Center for Clinical Research, University of Leipzig, Germany
[c] Centre for Endocrine and Diabetes Sciences, Cardiff University, UK

ARTICLE INFO

Article history:
Received 19 August 2010
Accepted 22 October 2010
Available online 28 October 2010

Keywords:
Thyroid autonomy
FRTL-5 cells
Iodine
Junb
Iyd
Apoptosis

ABSTRACT

Thyroid autonomy is a frequent cause of thyrotoxicosis in regions with iodine deficiency. Epidemiological data suggest that iodide may influence the course of pre-existing thyroid autonomy.
Making use of FRTL-5 cells stably expressing a constitutively activating TSH receptor mutation as an *in vitro* model of thyroid autonomy, we investigated the impact of iodide on proliferation, function and changes in global gene expression.
We demonstrate that iodine inhibits growth in TSHR WT and L629F mutant FRTL-5 cells and downregulates e.g. protocadherin cluster (Pcdha1–13) and thyroid responsive element (Thrsp). In addition functional genes e.g. iodotyrosine deiodinase (*iyd*) and oncogen junB are upregulated, while sodium-iodide-symporter (Nis) and thyroid peroxidase (Tpo) are downregulated by iodide.
Iodide tunes down the biological activity of autonomous thyrocytes and may thus be of therapeutic benefit not only to prevent the occurrence of somatic TSHR mutations, causing thyroid autonomy, but also to slow down the development of clinically relevant disease.

1. Introduction

Thyroid autonomy is defined as the TSH-independent function and proliferation of thyroid follicles [4,24]. The most frequent cause of thyroid autonomy are TSH receptor mutations, that cause a constitutive activation of the cAMP cascade resulting in stimulation of thyroid function and growth [11,20]. Thyroid autonomy is highly prevalent in geographic regions with iodide deficiency and rarely occurs in iodide-sufficient regions [15].

The link between thyroid autonomy and iodine deficiency is not ultimately clarified on the molecular level, however thyroid hormone synthesis requires H_2O_2 as a co-substrate, which very likely represents an important source of reactive oxygen species (ROS). *In vitro*, an increased mRNA expression of oxidative defense genes during iodine deficiency has been shown in thyroids of rat and mice [17]. Increased oxidative stress may lead to DNA damage and may promote mutagenesis e.g. the occurrence of gain-of-function TSHR mutations.

The impact of iodine on the further evolution of clonal thyroid autonomy to clinically relevant thyroid disease has not been studied on the molecular level so far. Iodine plays an important role in the regulation of thyroid growth and function. Supraphysiological doses of iodide have long been known to cause a temporary inhibition of thyroid hormone synthesis, a process termed the Wolff–Chaikoff effect, which is still used pre-operatively as "plummering" in some thyrotoxic patients. In addition, iodine excess has been shown to inhibit cell growth, induce apoptosis and affect cell morphology [25]. Hypothetically, iodine exposure might also suppress proliferation of autonomous thyrocytes thereby slowing the development of autonomous growth and preventing hyperthyroidism. Early support for such hypothesis comes from the Pescopagano survey of patients with known thyroid autonomy. In this study, hyperthyroidism occurred twice as frequent in the iodide deficient vs. the iodide-sufficient patient group, suggesting that iodide deficiency may indeed be a selection factor for the clinically relevant development of thyroid autonomy [2].

In this paper we expand on previous studies by the group of Ludgate et al. using an *in vitro* model of thyroid autonomy [3,11] and investigate iodine-induced changes in the transcriptome as well as its effects on regulation of cell growth and function in early stage thyroid autonomy compared to normal thyroid cells.

2. Material and methods

2.1. Cell culture conditions

We have studied the SB5 sub-clone of FRTL-5 cells stably expressing wild-type (WT) TSH receptor or 2 different gain-of-function TSHR mutants, L629F and A623I, introduced by retroviral infection as previously described [11]. FRTL-5 cells were maintained in a 2:1:1 mixture of DMEM (PAA Laboratories, Cölbe, Germany): Ham's F12 (PAA Laboratories, Cölbe, Germany): MCDB104 (GIBCO Life Technologies,

* Corresponding author. Department of Internal Medicine, Division of Endocrinology and Nephrology, University of Leipzig, Liebigstr. 18, 04103 Leipzig, Germany. Fax: +49 341 971 33 89.
E-mail address: Fuehrer@medizin.uni-leipzig.de (D. Führer).

0888-7543/$ – see front matter © 2010 Elsevier Inc. All rights reserved.
doi:10.1016/j.ygeno.2010.10.007

Karlsruhe, Germany) supplemented with 5% newborn calf serum (GIBCO Life Technologies, Karlsruhe, Germany), 10 µg/ml insulin, 0.4 µg/ml hydrocortisone (Calbiochem, San Diego, CA, USA), 45 µg/ml ascorbic acid (Sigma, Seelze, Germany), 5 µg/ml transferrin (Calbiochem, San Diego, CA, USA) and 5 mU/ml bovine TSH (Sigma, Seelze, Germany). Depending on the parameters analyzed, the cells were cultured in serum-containing medium, supplemented with TSH and varying concentrations of NaI (or NaCl) as indicated.

2.2. Direct cell counting

Cells were plated in complete (serum-containing) medium with or without TSH (1 mU/ml) in various iodide concentrations (1–50 mM NaI) in a density of 5×10^4 cells/well in 12-well plates. Cells were trypsinized on days 3, 6, 8 and 10, resuspended in phosphate buffered saline solution (PBS) and counted using a Neubauer counting chamber. Results are expressed as total counts per well. To monitor unspecific osmolaric effects of the salt solutions, sodium chloride was used in all experiments equivalent to the highest NaI concentration.

2.3. Apoptosis

Apoptosis was determined by staining cells with Annexin V-Cy5 (*Ex*/*Em* = 649 nm/670 nm). Annexin V is used to identify the externalization of phosphatidylserine during the progression of apoptosis and, therefore, is a marker for early phases of apoptosis. In brief, cells were incubated with 0–10 mM doses of sodium iodide for 72 h. Cells were washed twice with cold PBS, trypsinized and resuspended in 250 µl binding buffer (10 mM HEPES/NaOH pH 7.4, 140 mM NaCl, 2.5 mM CaCl2). 0.5 µl of Annexin V-Cy5 (PharMingen, San Diego, CA) and 10 µg propidium iodide was added to these cells prior to detection with a LSR II cytometer (Becton Dickinson UK Ltd, Oxford, Oxon, UK). Results were analyzed with FlowJo Software (Flow Cytometry Analysis Software; Tree Star, Inc., Leland Stanford, Jr. University).

2.4. Cell cycle analysis

FRTL-5 mTSHR cells cultured in complete medium with or without TSH and in the presence of varying NaI (0, 1 and 10 mM) concentrations, were plated in duplicates at a density of 3×10^5 cells/well in 6-well plates. After 72 h, trypsinized cells were washed in PBS and fixed in ice-cold 70% ethanol at 4 °C for 1 h, washed, then incubated in 250 µl PBS containing 50 µg/ml RNase for 30 min at 37 °C. Immediately prior to flow cytometry 10 µl of 1 mg/ml propidium iodide (Sigma) was added. In each case a minimum of 10,000 events were scanned on a LSR II flow cytometer (Becton Dickinson UK Ltd., Oxford, Oxon, UK). Results were analyzed with FlowJo Software (Flow Cytometry Analysis Software; Tree Star, Inc., Leland Stanford, Jr. University).

2.5. RNA extraction and quantitative real-time PCR

RNA extraction and cDNA synthesis were carried out as described and expression of the housekeeping gene *S6* was measured as a control in all samples by RT-PCR [9,10]. Real-time PCR (LightCycler system, LightCycler-DNA MasterSYBRGreen I kit; Roche, Mannheim, Germany) was performed using intron-spanning primers for slc5a5 (Nis), Tpo, Thrsp, Pcdha, Junb, Iyd and the housekeeping gene Rps6 (rat). For each PCR, annealing temperatures and $MgCl_2$ concentrations were optimized to create a one peak melting curve (primer sequences and PCR condition are available on request).

2.6. Microarray analysis

Before microarray analysis, RNA integrity and concentration was examined on an Agilent 2100 Bioanalyzer (Agilent Technologies, Palo Alto, CA, USA) using the RNA 6.000 LabChip Kit (Agilent Technologies) according to the manufacturer's instructions. Microarray analysis was conducted at the microarray core facility of the Interdisziplinäres Zentrum für klinische Forschung (IZKF) Leipzig (Faculty of Medicine, University of Leipzig). 3 µg of total RNA were used to prepare double-stranded cDNA (Superscript II, Life Technologies, Gaithersburg, MD USA) primed with oligo-dT containing an T7 RNA polymerase promoter site (Genset SA, Paris, France). cDNA was purified by phenol-chloroform extraction before *in vitro* transcription using the IVT labeling kit (Affymetrix, Santa Clara, CA, USA) to synthesize cRNA. The cRNA was fragmented and hybridized to Affymetrix Rat Genome, 230 2.0 arrays (Affymetrix, Santa Clara, CA, USA). Washing and staining of the probe array were performed according to the manufacturer's instructions. The array was scanned with a third generation affymetrix GeneChipScanner 3000.

Affymetrix GeneChip data representing approximately 30,000 transcripts with complete Rat Genome coverage were extracted from fluorescence intensities and were scaled in order to normalize data for inter-array comparison using MAS 5.0 software according to the instruction of the manufacturer (Affymetrix). Our GeneChip data are submitted to the Gene expression omnibus and to track under the accession number GSE22118 (http://www.ncbi.nlm.nih.gov/geo/).

Microarray experiments were conducted in duplicate. Data was filtered to remove genes with a lower than 2-fold change between experimental conditions. Genes were functionally categorized using NetAffx (Affymetrix; http://www.affymetrix.com), KEGG (http://david.abcc.ncifcrf.gov/), DAVID2008 (http://david.abcc.ncifcrf.gov/) and GenMapp (http://www.genmapp.org).

3. Results

3.1. Effect of iodide on proliferation in normal and autonomous FRTL-5 cells

The effect of 1 up to 50 mM iodide on proliferation of FRTL-5 cells stably expressing the WT TSHR, the mutant TSHR L629F or A623I were analyzed by cell counting in the presence and absence of TSH.

In Fig. 1A TSH-independent growth is shown for clones expressing the constitutively active TSHR mutations L629F and A623I. In absence of TSH, the highest cell numbers were found for A623I FRTL-5 cells. Similar to the previous study [11] the L629F FRTL-5 cells showed only a moderate increase in cell number. When cells were grown in the presence of TSH, similar increases in cell numbers were observed for all three FRTL-5 clones (WT TSHR, L629F and A623I mutant TSHR).

Addition of iodide inhibited proliferation in WT TSHR, L629F and A623I FRTL-5 cells irrespective of the presence or absence of TSH (Fig. 1B). Inhibition of proliferation was more pronounced in mutant TSHR cells compared to WT TSHR cells and increased with long-term iodide exposure (>72 h). Relative growth inhibition after treatment with 1 mM NaI reached 43%, 58%, and 88% in WT TSHR, L629F mTSHR and A623I mutant TSHR FRTL-5 cells, respectively (Fig. 1A).

3.2. Effect of iodide on apoptosis and necrosis in normal and autonomous FRTL-5 cells

To examine whether iodide mediated growth inhibition is due to apoptosis or necrosis flow cytofluorometric analysis of Annexin V-Cy5 and propidium iodide (PI) staining was performed after 72 h of iodide incubation in FRTL-5 cells over-expressing the L629F mTSHR or the WT TSHR (Fig. 2). Increased Annexin V labeling (= indicator of early apoptosis) was observed with increased iodide doses in WT and mutant TSHR FRTL-5 cells. Furthermore, increased iodide exposure was associated with increased Annexin V and PI (= indicator of late apoptosis) labeling indices, without differences for WT and mutant TSHR expressing FRTL-5 cells. In contrast, PI labeling indices (= indicator of necrosis) increased in

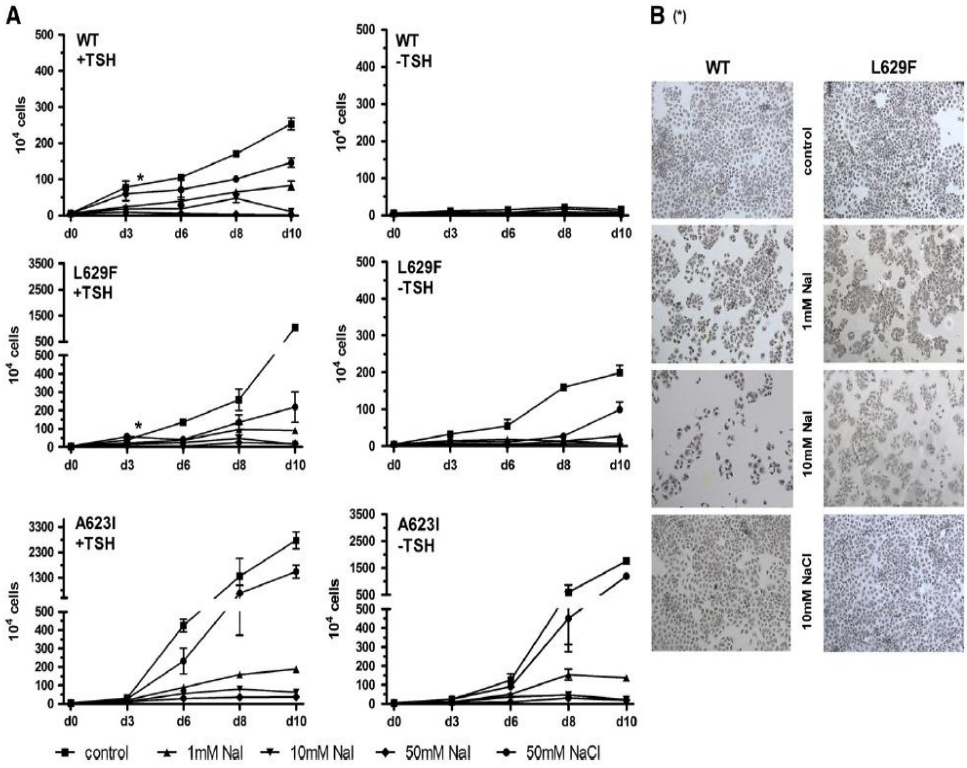

Fig. 1. Effects of iodide on cell proliferation in WT TSHR and mutant TSHR FRTL-5 cells (L629F and A623I mTSHR). Cell numbers were counted at day 3, 6, 8 and 10 after plating $5 * 10^4$ cells/well in 12-well plates in the presence or absence of TSH (control, black square). Iodide was added in 1 mM (black upward triangle), 10 mM (black downward triangle) and 50 mM (black rhombus) concentrations. To assess for tonicity effects sodium chloride was added in the highest iodide concentration (50 mM NaCl; black circle). (A) Dose dependent inhibition of iodide on cell growth. Three independent experiments were performed in duplicates. (B) Representative changes in cell numbers and morphology after 96 h stimulation with iodide in the presence of TSH in WT TSHR and L629F TSHR FRTL-5 cells (as assigned in (A) with *). NaCl in a concentration of 10 mM has no significant effect on proliferation unlike 50 mM NaCl (hematoxylin dye).

WT TSHR cells upon iodide exposure, while no increase in PI indices was found for L629F TSHR cells. This effect, however, was not significant.

These findings suggest that the lack of growth stimulation may be due to an increase of apoptosis in the presence of iodide.

3.3. Effect of iodide on cell cycle regulation in normal and autonomous FRTL-5 cells

To further assess, whether the lack of growth stimulation in cells stably expressing L629F or WT TSHR is associated with changes in cell cycle progression, cells were analyzed by flow cytometry after iodide exposure for 72 h. As shown in Fig. 3 iodide exposure results in a shift from G0/G1 to G2 phase in WT TSHR and L629F mTSHR FRTL-5 cells, which is less pronounced in L629F FRTL-5 cells and is accompanied by a S-phase reduction in these cells as previously shown by Al-Khafaji et al. [3]. This finding is in line with the known inhibitory effects of iodide on thyroid cell proliferation by causing G0/G1 and G2M arrest in high concentrations [22].

3.4. Effect of iodide on global gene expression in normal and autonomous FRTL-5 cells

To assess a broader spectrum of iodide effects on cell physiology, transcriptome profiles were obtained in the L629F and the WT TSHR FRTL-5 cell clones in the presence and absence of iodide, using microarray technology. Fig. 4 summarizes the number of genes and gene groups with at least 2-fold changes in the expression for iodide treated (1 mM NaI) vs. control (1 mM NaCl) WT TSHR and L629F mTSHR FRTL-5 cell clones.

To validate our GeneChip data we studied 6 iodine-regulated genes using quantitative real-time PCR (qPCR). With the main focus of genes involved in thyroid differentiation, we analyzed the thyroid peroxidase (Tpo), the thyroid hormone responsive element (Thrsp), the iodotyrosine deiodinase (Iyd) and the sodium-iodide symporter (Slc5a5/Nis). Differential regulation of the proto-oncogene jun B (Junb) was analyzed to validate a potential candidate with a focus on cell proliferation. In addition, Pcdha4 (protocadherin alpha 4) a member of the strongly regulated cadherin gene set was included in the qPCR validation. As shown in Fig. 5 quantitative real-time PCR analysis confirmed the reduction in mRNA expression in response to iodide in all investigated genes.

Using a cut-off of at least 2-fold expression difference our experiments showed iodide dependent upregulation of 6 genes (glucagon (Gcg), amphiregulin (Areg), ethanolamine kinase 1 (Etnk1), proline–serine–threonine phosphatase-interacting protein 1 (Pstpip1) and nuclear receptor interacting protein 3 (Nrip3) and downregulation of 68 genes (Table 3 — online supplement) in WT TSHR and L629F FRTL-5 cells.

Furthermore, comparison of gene expression pattern between L629F FRTL-5 cells and WT TSHR FRTL-5 cells in the presence of

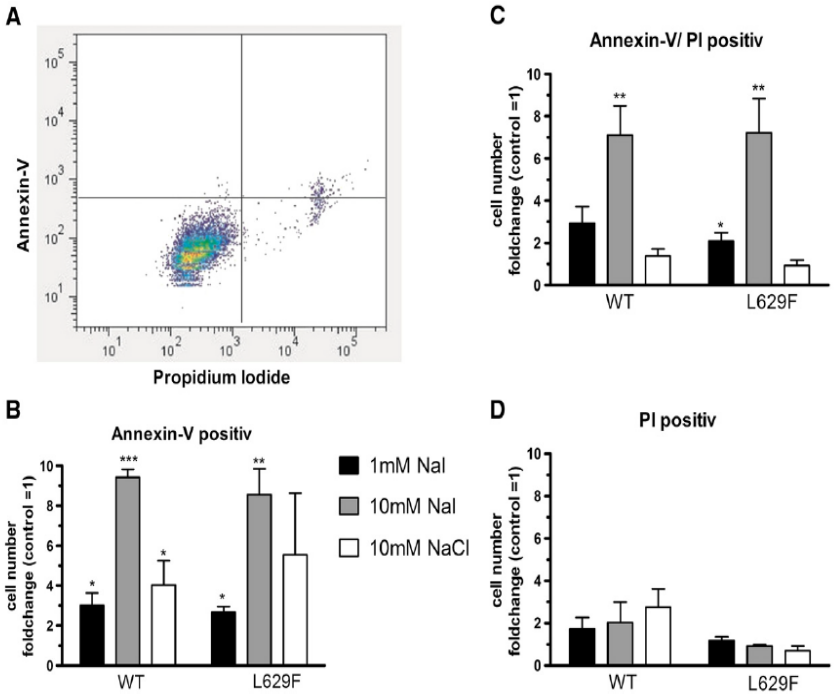

Fig. 2. Determination of apoptosis and necrosis using a flow cytometry based Annexin V assay. Cells treated with 1 mM, 10 mM NaI/ NaCl for 72 h, were stained with an anti-Annexin V antibody conjugated with Cy5 (ordinate). Propidium iodide (abscissa) was added before sorting. (A) Intact cells are located in the *lower left quadrant*, necrotic cells permeable to propidium iodide are shown in the *lower right quadrant*, apoptotic cells stained by Annexin V and propidium iodide are located in the *upper right and left quadrant*. (B) Iodine significantly upregulated apoptosis in WT TSHR and L629F mTSHR FRTL-5 cells. (C) Induction of iodine late apoptosis as demonstrated by Annexin V and propidium iodide labeling. (D) No significant induction of necrosis was seen by iodide exposure. Two different experiments were performed in triplicates.

1 mM NaI, showed 136 and 37 genes, which were up- and downregulated, respectively, between autonomous and normal thyroid cells (Table 3 – online supplement). Prominently upregulated genes in L629F cell clones were e.g. Rho GTPase activating protein 21 (Arhgap21), phosphatidylinositol-4-phosphate 5-kinase type 1 alpha (Pip5k1a), collagen type XII alpha 1 (Col12a1), ring finger protein 165 (Mf165) and neurotrophic tyrosine kinase, receptor, type 3 (Ntrk3) (Fig. 4A). Differentially downregulated genes in L629F cell clones were e.g. iodotyrosine deiodinase (Iyd), proto-oncogene jun B (JunB), tropomodulin 1 (Tmod1) and parvin alpha (Parva) (Table 3 – online supplement).

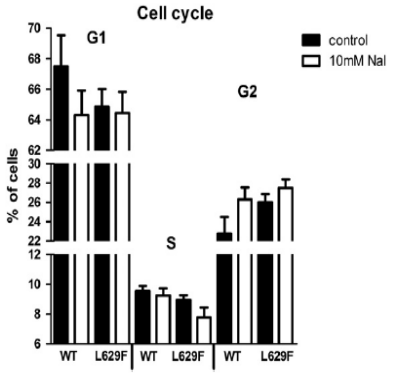

Fig. 3. Impact of iodide on cell cycle. L629F mTSHR and WT TSHR FRTL-5 cells were stimulated with 1 mM, 10 mM NaI or 10 mM NaCl in the presence of TSH for 72 h (data of 1 mM NaI and 10 mM NaCl are not shown). Subsequently, cells were stained with propidium iodide and were analyzed by flow cytometry. In both normal and autonomous thyroid cells iodine exposure induced a shift from G0/G1 to G2 phase without significant differences for 1 or 10 mM NaI. Values are the mean ± SD of two different experiments performed in triplicates.

When filtering genes with at least 1.5-fold expression difference using the DAVID2008 platform, the highest enrichment scores were obtained for categories of genes involved in cadherin signaling, cell adhesion, and ion binding (Table 1). Furthermore, analysis of microarray data by principal component analysis (PCA) showed a clear separation of the identified gene groups in WT vs. L629F TSHR FRTL-5 cells. Fig. 3B illustrates the PCA results comprising 74.6% of the identified genes with differential gene expression. The x-axis shows 36.8% difference in gene expression comparing WT and L629F FRTL-5 cells, while the y-axis shows 22.3% difference in iodide-induced gene expression. This illustrates, that the endogenous gene expression differences between autonomous thyrocytes (harboring the L629F TSHR mutation) and normal thyrocytes are more pronounced than effects of iodine on gene regulation. In other words, normal thyrocytes and autonomous thyroid cells are distinct molecular entities, with autonomy showing more impact on gene expression than iodine treatment. Iodine exposure affects both entities similarly but not identically. This finding is also illustrated by the total number of individually regulated genes (698 in WT clone versus 438 in L629F clone) and a total of only 74 genes, which are consistently regulated in normal and autonomous thyrocytes in response to iodide.

3.5. Effects of iodide on cell function in normal and autonomous FRTL-5 cells

Since iodide is known to inhibit thyroid function, besides proliferation, we were interested to investigate, whether this effect

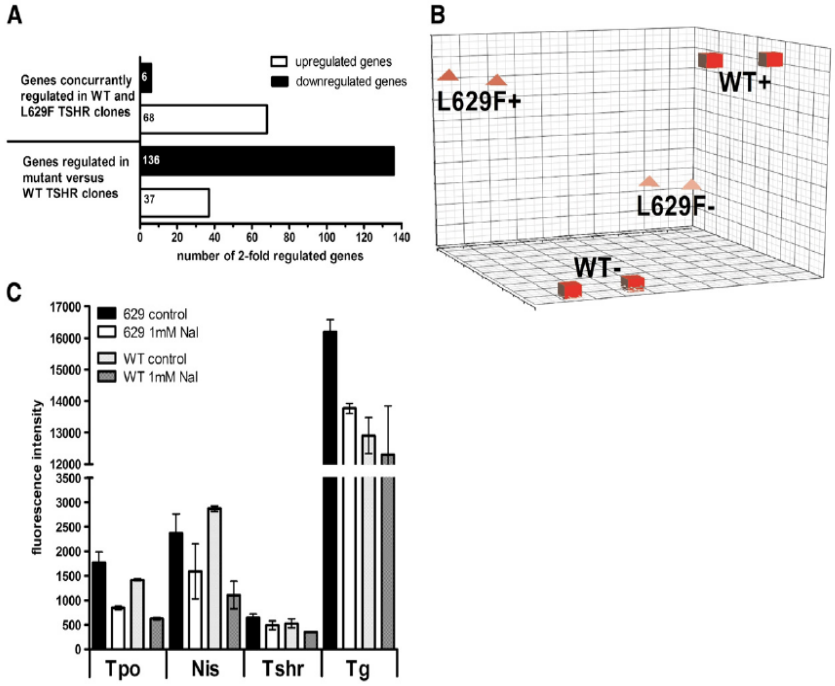

Fig. 4. Analysis of GeneChip data of L629F mTSHR and WT TSHR FRTL-5 cells in the presence and absence of 1 mM NaI. (A) Summary of upregulated genes (black bars) and downregulated genes (white bars) with at least 2-fold expression difference. Some genes are concurrently regulated in WT and L629F FRTL-5 cells. (B) 3-D visualization of a principal component analysis of the microarray data using Partek Genomics Suite software (Partek, St. Louis, MO, USA). (C) GeneChip data of thyroid differentiation genes. Fluorescence intensity of scan data of Tpo, Nis, Tshr and Tg in FRTL-5 hTSHR WT TSHR and L629F mTSHR FRTL-5 cells (control, black and bright shaded bars) and after 72 h 1 mM NaI treatment (white and dark shaded bars). Columns in the graph represent mean and SD values of two GeneChips per condition (WT/ L629F mutant). RNA extraction and array hybridization were performed in two different experiments.

also occurs in autonomously functioning thyrocytes and whether they react differently compared to normal thyrocytes.

Analysis of the sodium-iodide symporter and the thyroid peroxidase mRNA expression in WT TSHR FRTL-5 cells showed 1.5-fold downregulation (1.6-fold in 10 mM) and 3-fold downregulation (3.4-fold in 10 mM) in the presence of 1 mM iodide, respectively. In L629F TSHR FRTL-5 cells, incubation with 1 mM iodide resulted in 1.8-fold downregulation of Nis mRNA (2-fold in 10 mM) and in 3-fold downregulation of Tpo mRNA (3.5-fold in 10 mM) (Fig. 5B). Moreover, GeneChip analysis showed mRNA downregulation of other marker genes of thyroid function such as Tg and Tshr in WT and mutant TSHR FRTL-5 cells upon iodide exposure (Fig. 5C). Thus, iodide causes downregulation of thyroid function genes without significant difference between normal and autonomously functioning thyroid cells.

4. Discussion

Iodide is a pivotal factor in thyroid physiology and disturbed iodine homeostasis is an important trigger of thyroid pathophysiology. In this study we investigate an *in vitro* model of thyroid autonomy to determine the molecular effects of iodide on function, cell proliferation and global gene expression pattern in early stage autonomy.

We found reduced expression of genes important for thyroid function (Tpo, Nis, Thrsp, Iyd) in response to iodide exposure in normal and autonomously functioning FRTL-5 cell clones. Downregulation of functional genes has been reported in a recent SAGE analysis of the rat PCCl-3 cell line using similar iodide concentrations [16] and is in line with the Wolff–Chaikoff effect i.e. the inhibition of thyroid hormone synthesis and metabolism by iodide exposure [5,8].

Furthermore, in our experiments we observed an inhibition of cell proliferation in mutant and WT TSHR FRTL-5 cells clones, which was more pronounced in clones with constitutive TSHR activation and in the absence of TSH (i.e. the clinical equivalent of subclinical or overt hyperthyroidism). This effect has been reported in a previous study by Al-Kafahji et al. [3], but has now been demonstrated at much lower (1 mM) iodide concentrations. Further investigations showed that the reduction in growth is most likely due to increased apoptosis and G0/G1 and G2M arrest [22,23] with only marginal differences for WT TSHR and mutant TSHR cells. This could be due to the presence of TSH, which is a strong proliferation signal for thyrocytes. However, since the aim of our study was to assess the effect of iodide under physiological conditions we refrained from TSH deprivation of the investigated FRTL-5 cell clones.

Thus our *in vitro* data, which typify an artificial model however, suggest that iodide slows down growth and function in normal thyrocytes and early stage thyroid autonomy alike and may thus provide one explanation why thyroid autonomy is very rare in countries with iodide excess, e.g. Japan, despite the common molecular cause of activating TSHR mutations [13,19].

To get an insight into signaling events, which are altered by iodide, we performed global gene expression analysis using microarray technology.

Upon iodide exposure we found that a number of genes were simultaneously upregulated in WT TSHR and L629F mutant TSHR FRTL-5 cells. For example, upregulated genes included genes involved in cell cycle control (amphiregulin, Areg), cell metabolism (glucagon,

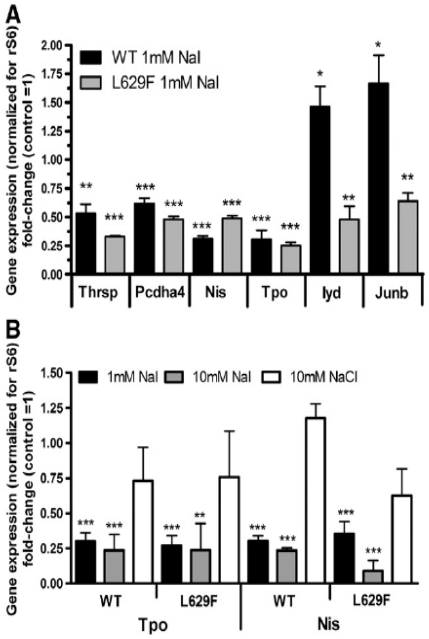

Fig. 5. Downregulation of thyroid function after iodide exposure and validation of expression difference by microarray analysis. (A) Quantitative Real-time PCR confirmation of GeneChip data. Iodide induced downregulation of *thrsp*, *pcdha4*, *nis*, *tpo*, *iyd* and *junb* was confirmed in WT TSHR and L629F TSHR FRTL-5 cells after 72 h treatment with 1 mM NaI. Data are presented as ratio of target mRNA normalized to the housekeeping gene ribosomal protein S6 and fold-change calculations to untreated control cells. (B) qPCR shows dose-dependent iodide-induced inhibition of *nis* and *tpo* mRNA expression in WT TSHR and L629F mutant TSHR FRTL-5 cells. Data are presented as fold-change of *nis* or *tpo* mRNA normalized to the housekeeping gene ribosomal protein S6 and untreated control cells. For all experiments cells were grown in the presence of TSH. The experiments were performed three times in duplicates.*$P<0.05$; **$P<0.01$; ***$P<0.001$ (ANOVA followed by Bonferroni's *post hoc* test and the Students t-test).

Gcg) and regulation of inflammatory processes (proline–serine–threonine phosphatase-interacting protein 1, Pstpip1).

In contrast, the complete gene cluster of protocadherin alpha was downregulated by iodide. We detected at least 13 highly similar coding sequences (Pcdha1-13) and two more distantly related coding sequences designated Pcdha c1 and Pcdha c2 in the Pcdha gene cluster, encoding N-terminal cadherin-like extracellular and transmembrane domains [26]. Those surface proteins are important in cell–cell adhesion [21]. A downregulation of this gene cluster could inhibit the cell–cell- and cell–surface adhesion and could reduce proliferation rate during iodide treatment.

In addition, downregulation of other genes involved in cell adhesion (laminin beta 3, Lamb3), cell metabolism (thyroid hormone responsive protein, Thrsp) and oxidative stress response (peroxidasin, Pxdn) underscore that iodide hampers cell viability in FRTL-5 cells.

Interestingly, more genes were found to be differential regulated by iodide in WT TSHR FRTL-5 cells compared to L629F mTSHR FRTL-5 cells. This could be due to the endogenous constitutive activity of the autonomous thyroid cells driving function and cell growth. However, of the distinctly regulated mRNAs between L629F TSHR and WT TSHR FRTL-5 cells three genes are worth highlighting due to their known relevance to thyroid physiology: i) iodotyrosine deiodinase (Iyd), ii) jun B proto-oncogene (Junb), and iii) the inhibitor of growth family, member 3 (Ing3). [14].

i) The iodotyrosine deiodinase (Iyd) also known as DEHAL1, facilitates iodide salvage in the thyroid cell thyroid by catalyzing the

Table 1
GeneChip data analysis using the DAVID2008 platform. Shown are the gene counts of the first annotation cluster with the highest enrichment score. Detailed information on differential gene expression in WT TSHR and L629F mTSHR FRTL-5 cells and influence of iodide on gene expression are available as a supplemental info (online Acc number GSE22118).

Gene group	Gene counts	P value
Cadherin, N-terminal	13	2,60E-23
Cadherin	13	4,20E-17
Cadherin repeats	13	3,50E-16
Homophillic cell adhesion	14	2,90E-15
Cell adhesion	15	2,90E-13
Cell–cell adhesion	15	9,70E-13
Biological adhesion	18	6,80E-11
Cell adhesion	18	6,80E-11
Calcium ion binding	17	2,20E-08
Calcium	15	4,70E-08
Cation binding	24	8,50E-05
Metal ion binding	24	1,90E-04
Ion binding	24	2,80E-04
Receptor	14	6,10E-03
Transmembrane	20	3,60E-02
Membrane	23	4,50E-02

NADPH-dependent deiodination of mono (L-MIT) and diiodotyrosine (L-DIT) [12]. Inactivating mutations in the *iyd* gene have been identified in rare cases of thyroid dyshormonogenesis [1,18]. Downregulation of Iyd suggests reduced iodide salvage at the level of thyroid hormone synthesis (in line with iodide-induced downregulation of thyroid hormone synthesis) but hypothetically could also present an advantageous escape mechanism for the autonomous cells from "inhibitory" iodide excess.

Junb mRNA is increased by e.g. TSH and insulin and is besides c-fos a necessary mediator and coordinator of growth response in thyroid epithelial cells [6]. The tumor suppressor ING3 acts as a cofactor of p53 and regulates cell cycle progression, apoptosis, and DNA repair [7]. Thus downregulation of Junb and Ing3 is compatible with a more pronounced inhibition of cell growth in autonomous L629F FRTL-5 cells compared to WT TSHR cells.

In summary, we show that distinct gene regulation occurs between normal and autonomous thyroid cells in response to iodide and affects genes involved in e.g. cell cycle, proliferation and metabolic processes. Importantly, despite a constitutive TSHR activation, iodide still causes downregulation of proliferation and function in early stage autonomy. Future studies need to address this issue in a scenario closer to the *in vivo* situation. Either by making use of primary cultures from toxic thyroid nodules or an animal model of thyroid autonomy. This may open novel perspective for the prevention of clinically relevant thyroid autonomy through iodide treatment.

Supplementary materials related to this article can be found online at doi:10.1016/j.ygeno.2010.10.007.

Duality of interest

The authors declare that there is no duality of interest associated with this manuscript.

Acknowledgment

This work was supported by a grant from the Interdisciplinary Center for Clinical Research Leipzig (Projects B26 and Z03) and by grant 107831 (to K.K.) from the Deutsche Krebshilfe.

References

[1] G. Afink, W. Kulik, H. Overmars, J. de Randamie, T. Veenboer, A. van Cruchten, M. Craen, C. Ris-Stalpers, Molecular characterization of iodotyrosine dehalogenase

deficiency in patients with hypothyroidism, J. Clin. Endocrinol. Metab. 93 (2008) 4894–4901.
[2] F. Aghini-Lombardi, L. Antonangeli, E. Martino, P. Vitti, D. Maccherini, F. Leoli, T. Rago, L. Grasso, R. Valeriano, A. Balestrieri, A. Pinchera, The spectrum of thyroid disorders in an iodine-deficient community: the Pescopagano survey, J. Clin. Endocrinol. Metab. 84 (1999) 561–566.
[3] F. Al Khafaji, M. Wiltshire, D. Fuhrer, G. Mazziotti, M.D. Lewis, P.J. Smith, M. Ludgate, Biological activity of activating thyrotrophin receptor mutants: modulation by iodide, J. Mol. Endocrinol. 34 (2005) 209–220.
[4] K. Bauch, Epidemiology of functional autonomy, Exp. Clin. Endocrinol. Diabetes 106 (Suppl 4) (1998) S16–S22.
[5] P.C. Clemens, R.S. Neumann, The Wolff–Chaikoff effect: hypothyroidism due to iodine application, Arch. Dermatol. 125 (1989) 705.
[6] S. Deleu, I. Pirson, F. Clermont, T. Nakamura, J.E. Dumont, C. Maenhaut, Immediate early gene expression in dog thyrocytes in response to growth, proliferation, and differentiation stimuli, J. Cell. Physiol. 181 (1999) 342–354.
[7] Y. Doyon, C. Cayrou, M. Ullah, A.J. Landry, V. Cote, W. Selleck, W.S. Lane, S. Tan, X.J. Yang, J. Cote, ING tumor suppressor proteins are critical regulators of chromatin acetylation required for genome expression and perpetuation, Mol. Cell 21 (2006) 51–64.
[8] P.H. Eng, G.R. Cardona, S.L. Fang, M. Previti, S. Alex, N. Carrasco, W.W. Chin, L.E. Braverman, Escape from the acute Wolff–Chaikoff effect is associated with a decrease in thyroid sodium/iodide symporter messenger ribonucleic acid and protein, Endocrinology 140 (1999) 3404–3410.
[9] M. Eszlinger, K. Krohn, K. Berger, J. Lauter, S. Kropf, M. Beck, D. Fuhrer, R. Paschke, Gene expression analysis reveals evidence for increased expression of cell cycle-associated genes and Gq-protein–protein kinase C signaling in cold thyroid nodules, J. Clin. Endocrinol. Metab. 90 (2005) 1163–1170.
[10] D. Fuhrer, M. Eszlinger, S. Karger, K. Krause, C. Engelhardt, D. Hasenclever, H. Dralle, R. Paschke, Evaluation of insulin-like growth factor II, cyclooxygenase-2, ets-1 and thyroid-specific thyroglobulin mRNA expression in benign and malignant thyroid tumours, Eur. J. Endocrinol. 152 (2005) 785–790.
[11] D. Fuhrer, M.D. Lewis, F. Alkhafaji, K. Starkey, R. Paschke, D. Wynford-Thomas, M. Eggo, M. Ludgate, Biological activity of activating thyroid-stimulating hormone receptor mutants depends on the cellular context, Endocrinology 144 (2003) 4018–4030.
[12] S. Gnidehou, B. Caillou, M. Talbot, R. Ohayon, J. Kaniewski, M.S. Noel-Hudson, S. Morand, D. Agnangji, A. Sezan, F. Courtin, A. Virion, C. Dupuy, Iodotyrosine dehalogenase 1 (DEHAL1) is a transmembrane protein involved in the recycling of iodide close to the thyroglobulin iodination site, FASEB J. 18 (2004) 1574–1576.
[13] H.I. Gozu, R. Bircan, K. Krohn, S. Muller, S. Vural, C. Gezen, H. Sargin, D. Yavuzer, M. Sargin, B. Cirakoglu, R. Paschke, Similar prevalence of somatic TSH receptor and Gsalpha mutations in toxic thyroid nodules in geographical regions with different iodine supply in Turkey, Eur. J. Endocrinol. 155 (2006) 535–545.
[14] M. Gunduz, M. Ouchida, K. Fukushima, S. Ito, Y. Jitsumori, T. Nakashima, N. Nagai, K. Nishizaki, K. Shimizu, Allelic loss and reduced expression of the ING3, a candidate tumor suppressor gene at 7q31, in human head and neck cancers, Oncogene 21 (2002) 4462–4470.
[15] P. Laurberg, K.M. Pedersen, H. Vestergaard, G. Sigurdsson, High incidence of multinodular toxic goitre in the elderly population in a low iodine intake area vs. high incidence of Graves' disease in the young in a high iodine intake area: comparative surveys of thyrotoxicosis epidemiology in East-Jutland Denmark and Iceland, J. Intern. Med. 229 (1991) 415–420.
[16] S.G. Leoni, P.A. Galante, J.C. Ricarte-Filho, E.T. Kimura, Differential gene expression analysis of iodide-treated rat thyroid follicular cell line PCCl3, Genomics 91 (2008) 356–366.
[17] J. Maier, H. van Steeg, C. van Oostrom, R. Paschke, R.E. Weiss, K. Krohn, Iodine deficiency activates antioxidant genes and causes DNA damage in the thyroid gland of rats and mice, Biochim. Biophys. Acta 1773 (2007) 990–999.
[18] J.C. Moreno, W. Klootwijk, H. van Toor, G. Pinto, M. D'Alessandro, A. Leger, D. Goudie, M. Polak, A. Gruters, T.J. Visser, Mutations in the iodotyrosine deiodinase gene and hypothyroidism, N Engl J. Med. 358 (2008) 1811–1818.
[19] E. Nishihara, N. Amino, K. Maekawa, H. Yoshida, M. Ito, S. Kubota, S. Fukata, A. Miyauchi, Prevalence of TSH receptor and Gsalpha mutations in 45 autonomously functioning thyroid nodules in Japan, Endocr. J. 56 (2009) 791–798.
[20] R. Paschke, M. Ludgate, The thyrotropin receptor in thyroid diseases, N Engl J. Med. 337 (1997) 1675–1681.
[21] L. Shapiro, A.M. Fannon, P.D. Kwong, A. Thompson, M.S. Lehmann, G. Grubel, J.F. Legrand, J. Als-Nielsen, D.R. Colman, W.A. Hendrickson, Structural basis of cell–cell adhesion by cadherins, Nature 374 (1995) 327–337.
[22] P. Smerdely, V. Pitsiavas, S.C. Boyages, Evidence that the inhibitory effects of iodide on thyroid cell proliferation are due to arrest of the cell cycle at G0G1 and G2M phases, Endocrinology 133 (1993) 2881–2888.
[23] P. Smerdely, V. Pitsiavas, S.C. Boyages, The G2M arrest caused by iodide is unrelated to the effects of iodide at adenylate cyclase, Thyroid 5 (1995) 325–330.
[24] G. Vassart, J.E. Dumont, The thyrotropin receptor and the regulation of thyrocyte function and growth, Endocr. Rev. 13 (1992) 596–611.
[25] M. Vitale, T. Di Matola, F. D'Ascoli, S. Salzano, F. Bogazzi, G. Fenzi, E. Martino, G. Rossi, Iodide excess induces apoptosis in thyroid cells through a p53-independent mechanism involving oxidative stress, Endocrinology 141 (2000) 598–605.
[26] Q. Wu, T. Maniatis, A striking organization of a large family of human neural cadherin-like cell adhesion genes, Cell 97 (1999) 779–790.

5.2 TSH compensates thyroid specific IGF-I receptor knockout and causes papillary thyroid hyperplasia

ORIGINAL RESEARCH

TSH Compensates Thyroid-Specific IGF-I Receptor Knockout and Causes Papillary Thyroid Hyperplasia

Kathrin Müller,* Dagmar Führer,* Jens Mittag, Nora Klöting, Matthias Blüher, Roy E. Weiss, Marie-Christine Many, Kurt Werner Schmid, and Knut Krohn

Department of Internal Medicine (K.M., D.F., M.B., K.K.), Division of Endocrinology, Diabetologia and Nephrology, Integrated Research and Treatment Center Adiposity Diseases (N.K.), and Interdisciplinary Center for Clinical Research (K.K.), University of Leipzig, Leipzig D-04103, Germany; Department of Cell and Molecular Biology (J.M.), Karolinska Institute, Stockholm S-17177, Sweden; Department of Medicine (R.E.W.), Section of Adult and Pediatric Endocrinology, Diabetes and Metabolism, The University of Chicago, Chicago, Illinois 60637; Universite Catholique de Louvain Medical School (M.-C.M.), Brussels B-1200, Belgium; and Institut of Pathology and Neuropathology (K.W.S.), University of Duisburg-Essen, Essen D-45122, Germany

Although TSH stimulates all aspects of thyroid physiology IGF-I signaling through a tyrosine kinase-containing transmembrane receptor exhibits a permissive impact on TSH action. To better understand the importance of the IGF-I receptor in the thyroid *in vivo*, we inactivated the *Igf1r* with a Tg promoter-driven Cre-lox system in mice. We studied male and female mice with thyroidal wild-type, *Igf1r*$^{+/-}$, and *Igf1r*$^{-/-}$ genotypes. Targeted *Igf1r* inactivation did transiently reduce thyroid hormone levels and significantly increased TSH levels in both heterozygous and homozygous mice without affecting thyroid weight. Histological analysis of thyroid tissue with *Igf1r* inactivation revealed hyperplasia and heterogeneous follicle structure. From 4 months of age, we detected papillary thyroid architecture in heterozygous and homozygous mice. We also noted increased body weight of male mice with a homozygous thyroidal null mutation in the *Igf1r* locus, compared with wild-type mice, respectively. A decrease of mRNA and protein for thyroid peroxidase and increased mRNA and protein for IGF-II receptor but no significant mRNA changes for the insulin receptor, the TSH receptor, and the sodium-iodide-symporter in both *Igf1r*$^{+/-}$ and *Igf1r*$^{-/-}$ mice were detected. Our results suggest that the strong increase of TSH benefits papillary thyroid hyperplasia and completely compensates the loss of IGF-I receptor signaling at the level of thyroid hormones without significant increase in thyroid weight. This could indicate that the IGF-I receptor signaling is less essential for thyroid hormone synthesis but maintains homeostasis and normal thyroid morphogenesis. (***Molecular Endocrinology*** **25: 1867–1879, 2011)**

Due to the strong negative symptoms associated with thyroid hormone imbalance, the activity of the thyroid gland is tightly controlled, mainly by the hypophyseal hormone TSH. However, other signaling cascades such as the IGF-I receptor (IGF-IR) are suspected to be very important as well, being part of a reciprocal permissive effect with TSH (1, 2).

IGF-IR activation by IGF-I or high concentration of insulin stimulates cell growth in particular by the activation of the rat sarcoma/rat fibrosarcoma/proto-oncogene B-RAF (BRAF) MAPK cascade and phosphatidylinositol 3-kinase (PI3K)/AKT pathway (3). Thereby it permits the mitogenic effect of TSH and cAMP. It was shown that mainly the type I IGFR is expressed in the thyroid gland (4). Overexpression of the IGF-IR together with IGF-I in the thyroid leads to an increase of gland weight and follicular lumen together with decreased TSH levels and increased serum T_4 concentrations, which suggest that

ISSN Print 0888-8809 ISSN Online 1944-9917
Printed in U.S.A.

doi: 10.1210/me.2011-0065 Received February 10, 2011. Accepted August 26, 2011.
First Published Online October 6, 2011

* K.M. and D.F. contributed equally to this study.

Abbreviations: BRAF, proto-oncogene B-RAF; EAT, epigonadal adipose tissue; GTT, glucose tolerance test; HEK, human embryonic kidney; HPT, hypothalamus-pituitary-thyroid; IGFIR, IGF-I receptor; INSR, insulin receptor; ITT, insulin tolerance test; NIS, sodium-iodide-symporter; PI3K, phosphatidylinositol 3-kinase; PVN, paraventricular hypothalamic nucleus; SSC, saline-sodium citrate; TG, thyroglobulin; TPO, thyroid peroxidase; TSHR, TSH receptor; WT, wild-type.

IGF-I and IGF-IR stimulate thyroid function (5). Moreover, a population-based study suggests that with higher serum IGF-I levels the odds for developing thyroid goiter increase (6). In thyroid carcinogenesis the IGF-I axis is a major regulator (7, 8). Follicular thyroid carcinomas often show deregulation in the PI3K pathway, which is a component of IGF-IR signaling. The PI3K/Akt/mammalian target of rapamycin pathway, which controls essential processes such as proliferation and survival, has recently emerged as a pivotal signaling cascade in follicular thyroid carcinoma development (9). Not only follicular thyroid carcinoma but also papillary thyroid carcinoma pathology is characterized by deregulation in MAPK signaling or mutations in the *PI3K* gene (10).

However, the physiological role of IGF-IR signaling in thyroid tissue *in vivo* has not been systematically studied. To investigate the role of the IGF-IR in the development and metabolism of the thyroid, we generated mice lacking the *Igf1r* in thyroid tissue using a conditional gene-targeting approach based on the Cre recombinase ($Igf1r^{TgCrc}$). Subsequently, we characterized the consequences of *Igf1r* deletion in thyroid tissue on morphological and metabolic parameters of $Igf1r^{TgCrc}$ mice.

The IGF and the structurally related insulin are essential for the control of embryonic and postnatal development. Through binding to its cell surface receptor, IGF stimulates the autophosphorylation of the receptor and activation of its intrinsic tyrosine kinase activity. In turn, this leads to the tyrosine phosphorylation of various intracellular substrates (11, 12). Conventional gene-targeting strategies used to abrogate IGF-IR signaling reveal severe phenotypes of *Igf1r*-deficient mice. Mice with a complete germline inactivation of the *Igf1r* gene die shortly after birth (13). Furthermore, heterozygous *Igf1r*-knockout mice have increased longevity, most likely due to greater resistance to oxidative stress (14). These data point to a role of IGF-IR signaling in the regulation of lifespan. Total ablation of the *Igf1r* or members of the *Igf* family in mice, shortly after birth, results in reduced body weight (11), brain growth retardation (15), muscle hypoplasia (16), and prolonged lifespan (14). To determine the relevance of IGF-IR signaling in individual tissues, mice with tissue-specific inactivation of the *Igf1r* have been created. Tissue-specific knockout of the *Igf1r* gene displayed several defects in specific organs and secondary effects on the organism (17–21). Tissue-specific knockout of the *Igf1r* gene in the white adipose tissue leads to increased IGF-I serum concentrations and *Igf1* mRNA levels in liver and adipose tissue combined with increased liver weight (22). However, despite the evidence for an important role of IGF-I in the thyroid, loss of IGF-IR signaling has not been investigated in this tissue to date.

Results

Conditional *Igf1r* knockout in the thyroid

Mice lacking one or two alleles of the *Igf1r* in thyrocytes ($Igf1r^{+/-}$ or $Igf1r^{-/-}$) were generated by crossing

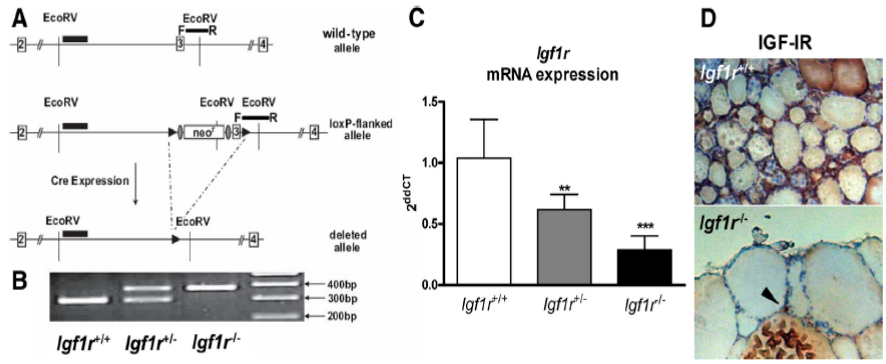

FIG. 1. Targeting strategy, assessment of *Igf1r* recombination, and *Igf1r* expression. A, Schematic representation of the WT (*upper panel*) and *loxP*-flanked *Igf1r* allele before (*middle panel*) and after (*lower panel*) recombination. Cre expression deletes exon 3 (*numbered box*) by recombination of the *loxP* sites flanking the *Igf1r* gene. F and R mark the location of the primers used in genotyping of tail biopsies. *EcoRV*, Restriction site; *filled triangle*, *loxP* site; *ellipse*, FRT site. B, Results from PCR analysis of DNA prepared from tail biopsies. DNA of WT mice produced a 300-bp band (lane 1), whereas a single 380-bp band was detected for *loxP*-flanked *Igf1r* allele (lane 3). Heterozygous expression of the transgene was detected by both a 300-bp and a 380-bp band (lane 2). C, Gene expression analysis of the *Igf1r* in the thyroid of WT, $Igf1r^{+/-}$, and $Igf1r^{-/-}$ mice (n = 10). Significant down-regulation of the *Igf1r* mRNA expression in heterozygous and knockout mice compared with the WT is evident in the 2^{ddCT} values of *Igf1r* normalized to the housekeeping gene *Hmbs*. **, $P < 0.01$; ***, $P < 0.001$. D, Immunohistochemistry with anti-IGF-IR-antibody in thyroid tissue of female WT ($Igf1r^{+/+}$) and $Igf1r^{-/-}$ mice. The *black arrowhead* marks a stained blood vessel among unstained thyrocytes in $Igf1r^{-/-}$ mice.

mice carrying the loxP-flanked *Igf1r* allele with transgenic mice expressing the Cre recombinase under control of the thyroid-specific thyroglobulin (*Tg*) promoter. The targeting strategy is shown in Fig. 1A. Mice with the $Igf1r^{flox/wt}$ or $Igf1r^{flox/flox}$ geneotype expressing Cre transgene were obtained close to the expected Mendelian frequency (data not shown). Because Cre expression was targeted to thyrocytes, detection of an $Igf1r^{flox}$ allele together with the Cre transgene in PCR analysis of the genomic DNA from tail biopsies results in loss of the allele in the thyroid. Hence, $Igf1r^{flox/flox}$ and $Igf1r^{flox/wt}$ mice that inherited the Cre transgene display $Igf1r^{-/-}$ and $Igf1r^{+/-}$ genotypes in thyrocytes, respectively. In fact, quantitative PCR analyses of reverse transcribed total RNA from thyroid showed significantly decreased *Igf1r* mRNA expression in knockout mice and strongly decreased mRNA expression in heterozygous mice (Fig. 1C). Furthermore, immunohistochemistry with an anti-IGF-IR antibody detects IGF-IR protein in $Igf1r^{-/-}$ only in cells other than thyrocytes (Fig. 1D). Western blot analysis of thyroid tissue lysates clearly indicated that IGF-IR protein was reduced in the thyroid of $Igf1r^{-/-}$ mice (Fig. 2A). No reduction of IGF-IR protein expression was found in the liver (Fig. 2A), brain, and skeletal muscle (data not shown).

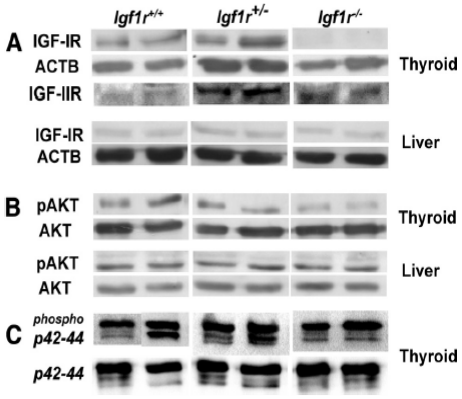

FIG. 2. Western blot analysis of proteins from WT ($Igf1r^{+/+}$), $Igf1r^{+/-}$, and $Igf1r^{-/-}$ mice. A, Thyroid-specific *Igf1r* knockout strongly reduces IGF-IR expression in thyroid but not in liver tissue of $Igf1r^{-/-}$ mice. In contrast, IGF-IIR protein is increased in thyroid tissue but not in liver of $Igf1r^{+/-}$ and $Igf1r^{-/-}$ mice compared with WT. β-Actin (ACTB) has been used as loading control. B, Activation of the AKT protein, a downstream signaling target of IGF-IR, is studied using a phosphorylation specific antibody (pAKT). Whereas expression of AKT is unchanged in thyroid and liver tissue of mice with different genotypes, phosphorylation of AKT is reduced in thyroids but not in liver of $Igf1r^{+/-}$ and $Igf1r^{-/-}$ mice. C, Activation of p42–44, a signaling target for several cell surface receptors that might play a role in the development of cancer. However, we do not detect differences of the expression of p42–44 as well as phosphorylated (phospho)-p42–44 in thyroids of $Igf1r^{+/-}$ and $Igf1r^{-/-}$ mice compared with WT.

Phenotype of *Igf1r*-knockout mice

Thyroid weight and follicle size

Thyroid weight of both female ($Igf1r^{-/-}$: 2.0 mg ± 0.5 *vs.* $Igf1r^{+/+}$: 1.7 mg ± 0.6) and male mice ($Igf1r^{-/-}$: 1.7 mg ± 0.5 *vs.* $Igf1r^{+/+}$: 2.1 mg ± 0.4), were not significantly different compared with wild-type (WT) littermates at the age of 4 months (Fig. 3A). As expected, thyroids of mice at the age of 1 y had a higher weight compared with the 4-month-old animals. However, we found no significant differences between knockouts and WT animals at the age of 1 yr (male $Igf1r^{-/-}$: 3.1 mg ± 0.6 *vs.* male $Igf1r^{+/+}$: 3.0 mg ± 0.3; female $Igf1r^{-/-}$: 3.2 mg ± 0.5 *vs.* female $Igf1r^{+/+}$: 2.8 mg ± 0.4).

Figure 2B illustrates the size distribution of thyroid follicles as a histogram. In knockout and heterozygous mice we detect a high number of very large follicles that exceeds the range of sizes in WT mice. Moreover, the medium size of thyroid follicles is significantly increased in knockout mice (+140%) as well as in mice with a deletion of one *Igf1r* allele (+130%) compared with $Igf1r^{+/+}$ (1547 μm^2 ± 1397).

Hormone level

Measurement of the thyroid hormones (Fig. 4) showed no significant change of serum T_3 levels at the age of 4 months and a slight increase of 41% of T_3 in 1-yr-old male mice, respectively. A significant decrease was detected for serum T_4 at 8 wk in male (−37%) and female (−36%) $Igf1r^{-/-}$ mice compared with WT. At 4 months and 1 yr T_4 levels of knockout animals are similar to those of WT mice, except for female knockout mice at 1 yr. TSH levels of $Igf1r^{-/-}$ and $Igf1r^{+/-}$ male and female mice (Fig. 5A) were significantly increased (male $Igf1r^{-/-}$: +754%, male $Igf1r^{+/-}$: +606% *vs.* male $Igf1r^{+/+}$: 131 mU/liter ± 53; female $Igf1r^{-/-}$: +933%, female $Igf1r^{+/-}$: +920% *vs.* female $Igf1r^{+/+}$: 30 mU/liter ± 15).

Bioactivity of TSH

Furthermore, cAMP accumulation was determined to analyze the bioactivity of serum TSH elevated in transgenic mice compared with WT mice (Fig. 5B). We used a cell model [human embryonic kidney (HEK) grip tide] with stable overexpression of the TSH receptor (TSHR) to test the sera of $Igf1r^{-/-}$, $Igf1r^{+/-}$, and WT mice for their ability to stimulate cAMP accumulation. Analyzing three sera of each genotype and sex, we found both sera of $Igf1r^{+/-}$ and $Igf1r^{-/-}$ mice to be able to induce cAMP accumulation in the cultured cells (male

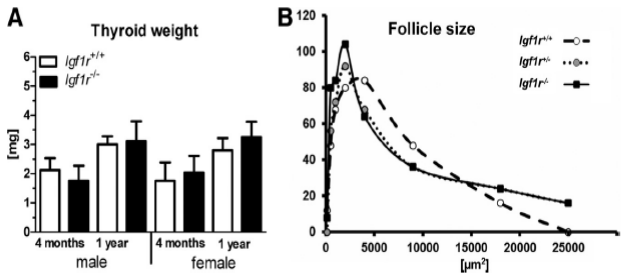

FIG. 3. Thyroid-specific *Igf1r* knockout only affects thyroid architecture. A, No significant changes in thyroid weight were detected in 4-month- and 1-yr-old male and female $Igf1r^{-/-}$ mice compared with WT mice. B, The *histogram* shows the distribution of the thyroid follicle size of the three genotypes. Knockout (*filled squares*) and heterozygous (*gray circles*) mice show a high number of very large follicles that are not present in WT mice (*open circles*). Follicle sizes were measured for three distinct thyroid sections of three knockout and three heterozygous as well as four WT mice of both genders.

$Igf1r^{-/-}$: +256%, male $Igf1r^{+/-}$: +152% *vs.* $Igf1r^{+/+}$: 14.1 nM ± 3.2; female: $Igf1r^{-/-}$: +189%, female $Igf1r^{+/-}$: +190% *vs.* $Igf1r^{+/+}$: 8.8 nM ± 1.7), suggesting that the circulating TSH is biologically active.

Thyroid hormone feedback

After ip injection of thyroid hormone in 6-month-old male and female $Igf1r^{-/-}$ and $Igf1r^{+/+}$ mice serum TSH fell below the detection level of our assay (Fig. 5C), which demonstrates an intact thyroid hormone feedback loop.

Insulin, IGF-I, and IGF-II

Measurement of the serum insulin and IGF-I level showed no significant change between WT and $Igf1r^{-/-}$ mice at the age of 4 months and 1 yr [insulin: 237 pM ± 33 ($Igf1r^{+/+}$; 4 month) *vs.* 261 pM ± 38 ($Igf1r^{-/-}$; 4 month) and 265 pM ± 34 ($Igf1r^{+/+}$; 1 yr) *vs.* 245 pM ± 34 ($Igf1r^{-/-}$; 1 yr) and IGF-I: 436 pM ± 36 ($Igf1r^{+/+}$; 4 month) *vs.* 486 pM ± 27 ($Igf1r^{-/-}$; 4 month) and 564 pM ± 53 ($Igf1r^{+/+}$; 1 yr) *vs.* 579 pM ± 33 ($Igf1r^{-/-}$; 1 yr)].

For serum IGF-II we detect a slight trend (not significant) for increased levels of knockout *vs.* WT mice at 4 months and 1 yr [1.10 nM ± 0.14 ($Igf1r^{+/+}$; 4 month) *vs.* 1.37 nM ± 0.27 ($Igf1r^{-/-}$; 4 month) and 0.93 nM ± 0.10 ($Igf1r^{+/+}$; 1 yr) *vs.* 1.07 nM ± 0.07 ($Igf1r^{-/-}$; 1 yr)].

mRNA expression

In addition to hormone levels we studied other functional markers of thyroid physiology that could be affected by loss of IGF-IR signaling (Table 1). mRNA expression of the respective transcripts were analyzed after normalization to the housekeeping gene *Hmbs*, which demonstrates very stable and ubiquitous expression in different tissues, is less sensitive to retardation of tissue asservation, and is not affected by experimental manipulation in thyrocytes (23, 24). Among transcripts relevant for thyroid physiology we found a significantly decreased (−66%) mRNA expression of thyroid peroxidase (*Tpo*) in female mice, whereas male mice showed only a slight decrease (−35%) of *Tpo* mRNA expression. We did not detect a significant alteration of sodium-iodide-symporter (*Nis*) and *Tg* mRNA expression (Table 1), underlining that the expression of the Cre transgene under the *Tg* promotor does not interfere with normal *Tg* expression.

Reduced or lost IGF-IR signaling could induce the expression of related receptors like IGF-IIR and insulin receptor (INSR). We observed an increased expression (up to +90%) of the *Igf2r* mRNA that is significant in female heterozygous and homozygous mice as well as in homozygous male mice (Table 1). In contrast, no significant change of expression was detected for the mRNA of the *Insr*. With an up to 10-fold increase of serum TSH in mice with loss of *Igf1r* we expected compensatory down-regulation of the *Tshr* mRNA. However, quantitative RT-PCR showed no change or slightly increased *Tshr* mRNA expression (Table 1).

IGF-IIR and signaling proteins

In addition to the expression of *Igf2r* mRNA, we used Western blot analysis to study the expression of the IGF-IIR protein (Fig. 2A). IGF-IIR protein is increased in the thyroid of both $Igf1r^{+/-}$ and $Igf1r^{-/-}$ compared with WT mice.

Furthermore, we focused on the expression and activation of AKT protein, which is a part of the IGF-IR signaling cascade. In Western blot analysis (Fig. 2B) we did not detect changes in AKT expression for the different genotypes. However, we demonstrate a down-regulation of activated/phosphorylated AKT protein in thyroid tissue with partial ($Igf1r^{+/-}$) or total loss of *Igf1r* expression in thyrocytes, which could be a direct effect of a loss of IGF-IR signaling. In contrast, we do not detect changes in the expression or activation of p42–44 ERK (Fig. 2C), which acts downstream of AKT but also mediates the signaling of other receptors (*e.g.* epidermal growth factor receptor).

BRAF sequencing

To look for a possible genetic alteration in the genome of cells from papillary structures we studied the *BRAF* gene in microdissected tissue of *Igf1r*-deficient mice and screened for mutations in the region equivalent to the

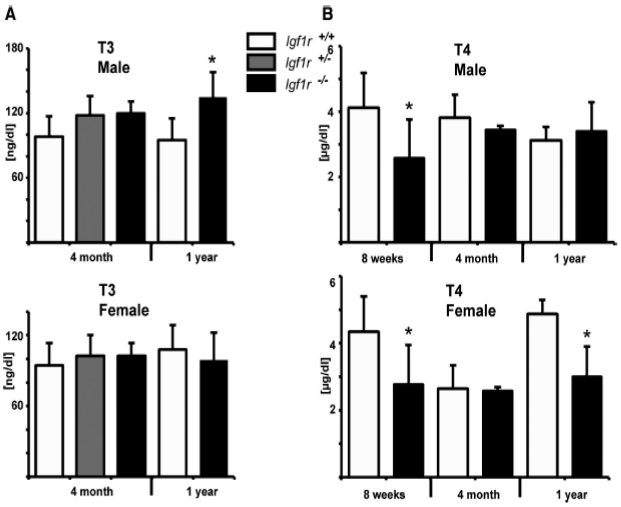

FIG. 4. Serum T_3 and T_4 concentrations of mice after *Igf1r* loss. A, Serum concentrations of T_3 of male (*upper graph*) and female (*lower graph*) mice at 4 months and 1 yr (n = 5). B, Serum T_4 concentrations of male (*upper graph*) and female (*lower graph*) mice at 8 wk, 4 months, and 1 yr (n = 5). A significant reduction of the T_4 level was detected in male and female knockout mice at 8 wk. *, $P < 0.05$.

human V600E mutation. However, in mRNA from eight dissected papillary structures from six mice we only detected WT BRAF sequences.

Histology

Thyroids of $Igf1r^{-/-}$ and $Igf1r^{+/-}$ are characterized by a profound alteration of thyroid architecture that is defined by an increase in heterogeneity. We detect a significant increase of medium follicle size as well as a number of very small follicles (Fig. 6). The most prominent findings are papillary structures both in $Igf1r^{-/-}$ and $Igf1r^{+/-}$ mice that strongly resemble papillary thyroid hyperplasia. They were detectable in 18/21 $Igf1r^{-/-}$ mice and three of three $Igf1r^{+/-}$ mice. One of the $Igf1r^{+/-}$ mice with papillary structures was studied at the age of 4 months, and the other two were studied at 1 yr. $Igf1r^{-/-}$ mice developed papillary thyroid architecture in 13/15 cases at the age of 1 yr, four of five cases at the age of 8 months, and one of one mice at 4 months since birth. None of the WT animals showed similar changes in thyroid morphology.

A thyroid marker protein involved in thyroid hormone synthesis is the TPO, which is identified with decreased levels in malignant thyroid tissue, *e.g.* papillary thyroid carcinomas (25). We detect a reduced expression of the *Tpo* mRNA in mice with targeted Igf1r loss (Table 1). Immunohistological staining for the TPO protein in $Igf1r^{-/-}$ and $Igf1r^{+/-}$ mice showed a reduction in the papillary regions compared with the WT and the normal thyroid tissue (Fig. 7A). An alteration in the normal thyroid tissue of $Igf1r^{-/-}$ and $Igf1r^{+/-}$ mice compared with the WT was not detectable.

For other thyroid markers such as NIS, we found homogenous stained thyrocytes in $Igf1r^{-/-}$, $Igf1r^{+/-}$, and $Igf1r^{+/+}$ mice (Fig. 7B). The same is seen for TG staining (Fig. 7C). There is no visible difference in the intensity of the stained follicle with normal architecture between the transgenic and WT mice. To detect changes in the iodination status of follicular TG, thyroids were stained with a T_4-TG antibody. As shown in Fig. 7D. thyroids of both $Igf1r^{-/-}$ and $Igf1r^{+/-}$ mice contained tetra-iodinated thyroxyl residues in the TG protein in their follicles, which indicates normal thyroid hormone synthesis.

Caspase-3 staining

To study the consequences of targeted *Igf1r* inactivation on apoptosis we stained thyrocytes in $Igf1r^{-/-}$ and $Igf1r^{+/+}$ mice with an antibody against activated caspase-3 (Asp175). Activation of caspase-3 is an important marker of cellular apoptosis induced by a wide variety of apoptotic signals (26). An index of stained to all follicular thyrocytes was calculated in three slices of three WT and three $Igf1r^{-/-}$ mice. In thyroid tissue of *Igf1r*-deficient mice we detect a reduced index (−56%; 4.5% ± 5.3) compared with WT mice (10.2% ± 3.7).

Hypothalamus-pituitary-thyroid axis

To study the status of the hypothalamus feedback regulation, we determined the transcript levels of *TRH* (*Trh*) a target gene of thyroid hormone action in the paraventricular hypothalamic nucleus (PVN) of the hypothalamus. Within the negative-feedback loop of the hypothalamus-pituitary-thyroid (HPT) axis, *Trh* mRNA expression in the PVN is inversely correlated to thyroid hormone levels and thus represents a suitable sensor of intracellular T_3 content. Compared with WT animals, *Trh* transcript levels were 18% up-regulated in PVN neurons of $Igf1r^{-/-}$ mice ($Igf1r^{-/-}$: 13.4±1.9 *vs.* $Igf1r^{+/+}$: 11.3 ± 1.0, $P = 0.13$) (Fig. 8). The slightly elevated *Trh* mRNA levels in the PVN of $Igf1r^{-/-}$ mice prompted us to analyze other components of the HPT axis. However, D2 transcript levels in hypothalamic tanycytes of $Igf1r^{-/-}$ mice were not affected by the *Igf1r* knockout ($Igf1r^{-/-}$: 16.8 ± 1.4 *vs.* $Igf1r^{+/+}$: 18.2 ± 5.3, $P = 0.35$) (Fig. 8).

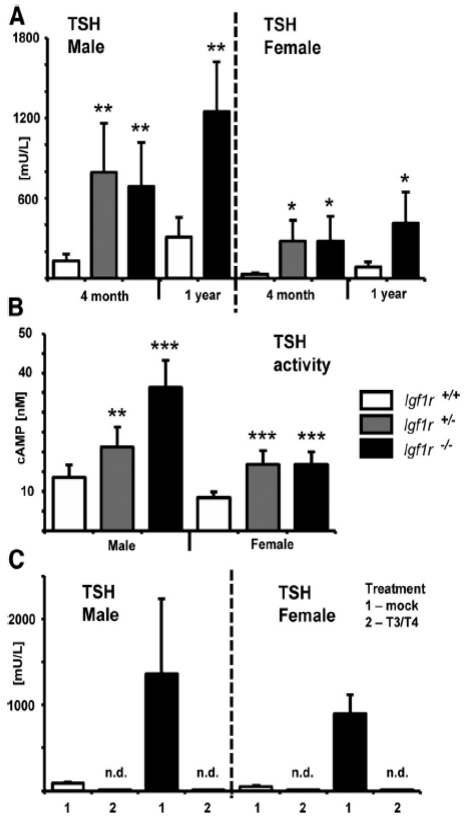

FIG. 5. Serum TSH concentration and activity of serum TSH of mice after *Igf1r* loss. A, Strong increase of serum TSH in male and female mice with homozygous and heterozygous loss of *Igf1r* in thyroid tissue at 4 months and 1 yr. B, Increased cAMP concentrations in HEK hTSHR cells stimulated with $Igf1r^{+/-}$ and $Igfr1^{-/-}$ sera compared with $Igf1r^{+/+}$ indicate biologically active TSH. Sera of three mice per genotype were measured in triplicates in two independent experiments. C, Serum TSH reaches levels below the detection limit after injection of a T_3/T_4 mixture in WT and $Igf1r^{-/-}$ mice compared with mock injection. n.d., Not detectable; *, $P < 0.05$; **, $P < 0.01$; ***, $P < 0.001$.

Body weight

At the age of 4 months, $Igf1r^{-/-}$ male mice exhibit a 10% increase ($Igf1r^{-/-}$: 32.5 g ± 6.2 *vs.* $Igf1r^{+/+}$: 27.8 g ± 1.1) in body weight compared with $Igf1r^{+/+}$ mice (Fig. 9A). These differences were amplified at the age of 1 yr, when $Igf1r^{-/-}$ male mice exhibited a 22% body weight increase ($Igf1r^{-/-}$: 43.8 g ± 5.6 *vs.* $Igf1r^{+/+}$: 35.7 g ± 2.2). Although these gains in body weight in male mice are consistent with a latent hypothyroidism, we unexpectedly saw a body weight decrease in female $Igf1r^{-/-}$ mice at the age of 4 months ($Igf1r^{-/-}$: 20.9 g ± 0.6 *vs.* $Igf1r^{+/+}$: 25.2 g ± 3.3) and 1 yr ($Igf1r^{-/-}$: 25.3 g ± 3.7 *vs.* $Igf1r^{+/+}$: 35.9 g ± 6.8).

Epigonadal adipose tissue (EAT) weight

A similar distribution is seen in the relative EAT weight (calculated as percentage of the whole body weight, Fig. 9B). At the age of 4 months $Igf1r^{-/-}$ male and female mice exhibit 81% increased ($Igf1r^{-/-}$: 2.0 g ± 0.8 *vs.* $Igf1r^{+/+}$: 1.1 g±0.3) and 13% decreased ($Igf1r^{-/-}$: 0.7 g ± 0.2 *vs.* $Igf1r^{+/+}$: 0.8 g ± 0.2) EAT weight, respectively (Fig. 9B). However, the heterozygote littermates show no differences compared with the WT. Those differences were not observed in male mice at the age of 1 yr, where $Igf1r^{-/-}$ male and female mice exhibited 8% decreased ($Igf1r^{-/-}$: 3.9 g ± 1.4 *vs.* $Igf1r^{+/+}$: 4.2 g ± 1.1) and 55% decreased ($Igf1r^{-/-}$: 1.8 g ± 1.2 *vs.* $Igf1r^{+/+}$: 4.0 g ± 2.2) EAT weight, respectively (Fig. 9B).

Metabolic effects of the thyroid-specific *Igf1r* knockout

Igf1r-specific knockout in adipose tissue revealed alterations in insulin tolerance tests (ITT) and glucose tolerance tests (GTT) (22). To determine the physiological consequences of reduced thyroid specific *Igf1r* expression on metabolic parameter glucose, we also performed ITT and GTT at the age of 3 months. Intraperitoneal ITT showed low insulin resistance in male and no changes in female $Igf1r^{-/-}$ mice compared with control mice (data not shown). Intraperitoneal GTT demonstrated normal glucose tolerance in male and female $Igf1r^{-/-}$ and control mice (data not shown).

Neurological effects of the *Igf1r* knockout

Alterations in the thyroid hormone status often cause behavioral abnormalities, *e.g.* anxiety and depressive and cognitive disorders (27, 28). To test for locomotor deficiencies or anxiety-like behavior, we performed the open-field test, which is a basic test of behavioral phenotyping for motional and emotional behavior (29). We found reduced entered field numbers in $Igf1r^{-/-}$ mice ($Igf1r^{-/-}$ +30% *vs.* $Igf1r^{+/+}$: 18.5 fields/min ± 4.9, n = 6) with no difference regarding which fields were entered (corner, bolder, or middle field). Therefore, $Igf1r^{-/-}$ mice show no abnormal anxiety but reduced activity compared with the WT mice. To further analyze the reduced motional attendance of $Igf1r^{-/-}$ mice, we placed them at the age of 15 wk for 7 d in wheel cages. Male $Igf1r^{-/-}$ mice exhibit significantly reduced rotations over a period of 7 d ($Igf1r^{-/-}$ −47% *vs.* $Igf1r^{+/+}$: 3074 ± 829 rotations per day, n = 7). The female knockout mice showed just an akin motional attendance compared with control animals.

Discussion

Our study, for the first time, describes the consequences of thyroid-specific loss of IGF-IR signaling. Our genetic

TABLE 1. Gene expression analyses in WT, *Igf1r*$^{+/-}$ and *Igf1r*$^{-/-}$ thyroids of one year old male and female mice

	Tg			*Nis*			*Tpo*			*Igf2r*			*Tshr*			*Insr*		
	Mean	±SD	n	Mean	±SD	n	Mean	±SD	n	Mean	±SD	n	Mean	±SD	n	Mean	±SD	n
Igf1r $^{+/+}$, m	**1.00**	0.32	4	**1.00**	0.28	5	**1.00**	0.22	4	**1.00**	0.15	5	**1.00**	0.31	5	**1.00**	0.20	5
Igf1r $^{+/-}$, m	**0.81**	0.48	5	**1.07**	0.30	5	**0.65**	0.07	5	**1.28**	0.20	5	**1.75**	0.24	5	**0.75**	0.14	5
Igf1r $^{-/-}$, m	**0.74**	0.33	5	**1.41**	0.13	5	**0.80**	0.10	5	**1.78**[a]	0.14	5	**1.97**	0.84	5	**1.19**	0.12	5
Igf1r $^{+/+}$, f	**1.00**	0.44	4	**1.00**	0.25	7	**1.00**	0.07	5	**1.00**	0.08	5	**1.00**	0.08	5	**1.00**	0.06	5
Igf1r $^{+/-}$, f	**1.36**	0.72	5	**0.83**	0.12	5	**0.42**[a]	0.08	5	**1.93**[b]	0.43	5	**1.20**	0.26	5	**1.03**	0.27	5
Igf1r $^{-/-}$, f	**1.02**	0.29	4	**0.64**	0.27	6	**0.33**[c]	0.05	4	**1.58**[c]	0.18	4	**0.96**	0.38	4	**1.00**	0.13	4

Analyzed are the *Tg*, *Nis*, *Tpo*, *Igf2r*, *Tshr*, and *Insr* mRNA expression levels with Taqman probe kits from Applied Biosystems. Shown are the means of 2^{-ddCT} values of the respective gene (no *bold*) normalized to the housekeeping gene *Hmbs* compared to the WT mice. Student's *t* test was performed per genotype and sex ($P < 0.05$ was considered significant). [a] $P < 0.01$; [b] $P < 0.01$; [c] $P < 0.001$. f, Female; m, male.

mouse model disrupts the expression of the *Igf1r* gene in the thyroid and thereby allows the dissection of normal extrinsic thyroid stimulation and gives important insights into thyroid growth regulation. Although thyroid weight appeared normal, we detected a transient decrease of serum T_4 at 8 wk, which returned to a normal level from 4 month on together with a tremendous increase in serum TSH. Moreover, the strong increase of serum TSH can be abolished by exogenous thyroid hormone treatment, which suggests that the thyroid hormone feedback is functioning normally.

Reduced serum T_4 at 8 wk indicates early transient hypothyroidism, which later classifies as subclinical hypothyroidism characterized by normal thyroid hormone and high TSH together with the symptoms of weight gain and reduced activity. Increased body and EAT weight, as well as reduced motional attendance, would be the typical

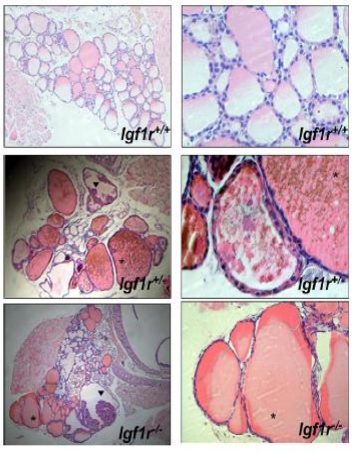

FIG. 6. Hematoxylin and eosin-stained thyroid slices of 1-yr-old mice at low (*right panel*) and high magnifications (*left panel*). The *upper panels* show a male WT mouse. *Igf1r* knockout (*lower panel*, male) and heterozygous (*middle panel*, female) mice show a heterogeneous follicle structure with very large follicles (*stars*). *Igf1r*$^{+/-}$ and *Igf1r*$^{-/-}$ mice developed papillary thyroid architecture (*arrowheads*) resembling papillary hyperplasia.

results of such a classification which perfectly applies to male mice with *Igf1r* loss. Unexpectedly, we detected a reversed metabolic phenotype in females. This is not easily explained, and at present we cannot exclude for instance that a subtle phenotype of the pregnant *Tg* Cre mothers interferes with the fetal programming of the metabolic setpoint, an epigenetic mechanism known to lead to a sexual dimorphism in offspring metabolism.

However, the thyroid histology of all mice with loss of *Igf1r* is very similar but not completely in line with human latent hypothyroidism, which is histologically dominated by signs of autoimmune disease. In fact, thyroid weight is normal, and histology reveals great heterogeneity with foci of papillary structures. These structures present as papillary thyroid hyperplasia because we did not detect evidence of capsular or vascular invasion and did not detect BRAF mutations frequently seen in human papillary carcinoma. Papillary structures are already detectable at 4 months and reach a frequency of about 86% in mice with complete loss of the *Igf1r* alleles. Importantly, we see papillary thyroid architecture with a similar frequency also in mice with loss of one *Igf1r* allele. This strongly suggests that this pathological histology is the result of a gene dosage effect of the IGF-IR and could also be related to the strong increase in serum TSH. However, nontransgenic mice treated with antithyroid drugs to cause hypothyroidism along with high TSH levels rarely develop thyroid cancer (30). In contrast, transgenic mice with chronic cAMP stimulation develop papillary growth but show signs of papillary cancer only very late (31). Moreover, a correlation between TSH and risk of papillary thyroid cancer in patients with nodular thyroid disease has been reported (32). The underlying mechanism could involve activation of the MAPK pathway stimulated by strongly elevated serum TSH levels as discussed by Nikiforov (33). On the level of TSHR signaling such positive cross talk between the TSH/cAMP and MAPK/ERK pathways could result from activation of G protein subunits $\beta\gamma$ and involve the PI3K pathway (34). More-

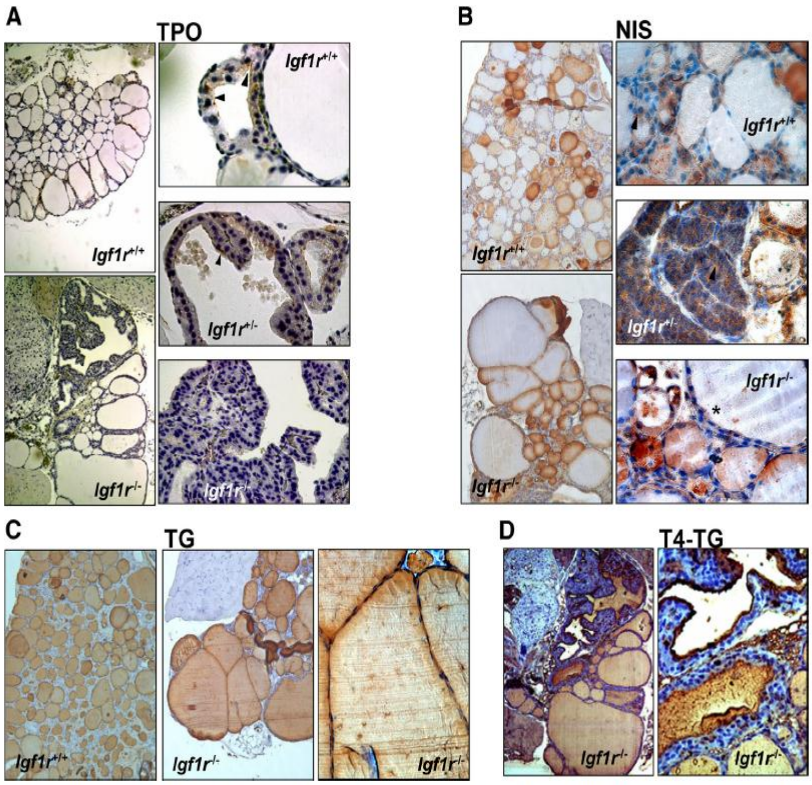

FIG. 7. Immunohistological staining of 1-yr-old male *Igf1r*$^{+/+}$, female *Igf1r*$^{+/-}$, and male *Igf1r*$^{-/-}$ mice at low and high magnifications. Thyroids were stained with antibodies against TPO (A), NIS (B), TG (C), and T_4-TG (D). A, There is no difference in the TPO staining of normal thyroid tissue between *Igf1r*$^{+/+}$ and *Igf1r*$^{-/-}$ mice (*arrowheads, upper and middle right panel*), whereas the papillary hyperplasia in *Igf1r*$^{-/-}$ (*lower right panel*) shows only slight TPO staining. B, NIS staining is detected not only in the follicular structures of small and large follicles (*star, lower right panel*) but also in the papillary structures (*arrowhead, middle right panel*). C, Homogenous TG-stained thyrocytes in *Igf1r*$^{+/+}$, *Igf1r*$^{-/-}$ mice and magnification of a stained large follicle (*right panel*). D, Thyroids of both *Igf1r*$^{+/+}$ and *Igf1r*$^{-/-}$ mice contained tetraiodinated TG in their follicles.

over, in our mice, elevation of TSH is very likely high enough to also stimulate the cAMP-independent Gq signaling of the TSHR (35). However, we do not detect changes in the expression or activation of p42–44 ERK protein, which is central to the signaling cross talk mentioned above. Therefore, the very early development of papillary thyroid lesion might result from TSH stimulation in an unexpected way. However, high TSH might rather support the progression of a preexisting lesion (36). If and how disruption of IGF-I signaling causes the primary lesion is still unknown. But another hypothesis for the development of papillary structures comes from *in vitro* studies with embryonic stem cells. As shown by Arufe *et al.* (37) the differentiation of murine stem cells into thyrocytes depends on IGF-I and IGF-IR. Therefore, aberrant differentiation caused by loss of *Igf1r* could be the cause of the papillary structures. However, the coexistence of both normal and papillary thyroid architecture in our model suggests that there is at least partial compensation by other growth factors that might not be present in an *in vitro* setting or the papillary growth is caused by an additional lesion.

Furthermore, our model produces an unexpected outcome concerning the HPT axis. Normally TSH production in the thyrotroph of the hypophysis is regulated by feedback inhibition through circulating thyroid hormone and via stimulation by hypothalamic TRH (38). Because our mice with loss of *Igf1r* expression in the thyroid have normal or even slightly elevated thyroid hormone levels and *in situ* hybridization in the PVN shows normal TRH expression, a normal serum TSH would be expected. However, we detected an increase of serum TSH in both the *Igf1r*$^{-/-}$ and the *Igf1r*$^{+/-}$ mice in the range of 6- to 9-fold. One plausible explanation could be reduced bioactivity of the TSH (39) produced in transgenic animals. However, our sensitive cell model-based assay with stable

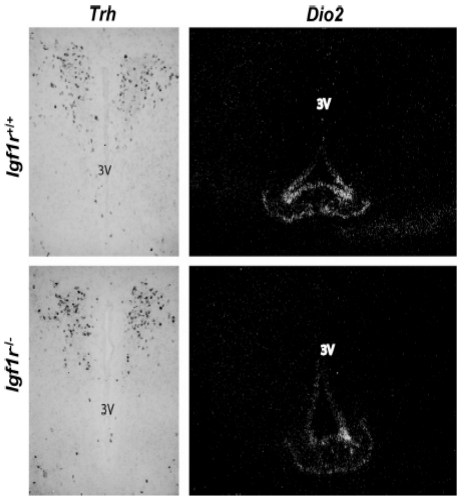

FIG. 8. *In situ* hybridization of the *Trh* and *Dio2* gene in the hypothalamic region of female WT and *Igf1*$^{-/-}$ mice.

overexpression of the TSHR indicated very strong cAMP accumulation in response to sera of *Igf1r*$^{-/-}$ and *Igf1r*$^{+/-}$ compared with WT mice. Although the mode of regulation is unknown, we hypothesize that elevated functionally active TSH compensates for the loss of IGF-I signaling in respect to thyroid hormone production.

The loss of IGF-I signaling is conditionally targeted to the thyroid with a *Tg* Cre expression system. As a result, one or two alleles of *Igf1r* are lost in differentiated thyrocytes. Hence, we detect a decrease of *Igf1r* mRNA in thyroid tissue of heterozygous mice and a further loss of mRNA in mice with loss of both *Igf1r* alleles. The latter show remaining *Igf1r* mRNA expression from cells other than thyrocytes (*e.g.* c-cells, fibroblasts, endothelial cells) that do not activate the *Tg* promoter. Furthermore we see a concurrent down-regulation of activated AKT protein, which is a major regulator of the downstream insulin cascade and has been shown *in vitro* by Zhang *et al.* (40). The *Tg*-targeted *Cre* system has been used for thyroid-selective gene expression in many transgenic studies (41). Recently it was used to impair the Gq/G11-signaling cascade of the TSHR and to cause IGF-IR overexpression (5, 42). Furthermore, in a mouse model of Zeiger *et al.* (31) the *Tg* promoter gene has been used for the thyroid-specific overexpression of the choleratoxin A gene.

Although increased TSH stimulation might keep thyroid hormone levels in a normal range, the loss of *Igf1r* signaling could lead to other systemic or local compensation that would maintain homeostasis. However, we did not detect changes of serum insulin and IGF-I level. At the level of mRNA expression we detected increased expression of the *Igf2r* in thyroid tissue of *Igf1r*-deficient mice whereas the insulin receptor and the *Tshr* mRNA are unchanged compared with WT mice. Unchanged expression of the *Tshr* mRNA is an especially unexpected outcome because high levels of bioactive serum TSH mean a very strong stimulus for thyrocytes that could lead to down-regulation of *Tshr* mRNA expression. However, gene expression analysis of primary thyrocytes did not detect TSHR as differentially down-regulated by TSH treatment (23). Moreover, recent work by Moeller *et al.* (43) implies that the TSHR expression level is set by the thyrocyte and not in response to settings of the HPT loop. Moreover, we detect a reduced mRNA expression of *Tpo* that is more difficult to interpret considering normal serum level of thyroid hormones. However, this reduction very likely reflects the observation that papillary structures hardly express TPO (Fig. 7A) and thereby dilute TPO expression of normal thyroid tissue due to RNA preparation from whole thyroid glands.

In addition to the increase of *Igf2r* mRNA the expression of the IGF-IIR protein is also increased. Moreover there is also a slight but not significant increase of serum IGF-II. Together this suggests that in addition to TSH part of the compensatory effect could be attributed to IGF-II signaling.

Our model fits perfectly with results from the reverse mice model: overexpression of the IGF-IR together with IGF-I in thyroid tissue (5). The latter mice develop goiter and show reduced serum TSH level and slightly increased T_4. This could indicate that IGF-IR signaling is less essential for thyroid hormone synthesis but maintains homeostasis and normal thyroid morphogenesis. Our results further suggest that the strong increase of TSH benefits papillary growth and, together with a moderate increase of the IGF-IIR, completely compensates the loss of IGF-IR signaling at the level of thyroid hormones without a

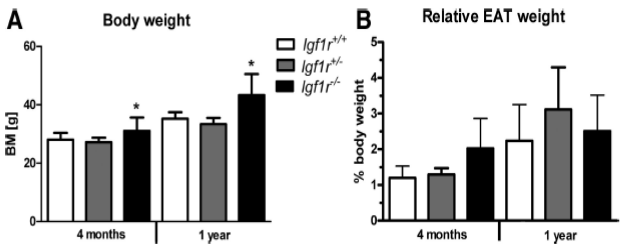

FIG. 9. Consequences of thyroid-specific *Igf1r* knockout on body composition of male mice. A, Body weight of 4-month- and 1-yr-old male *Igf1*$^{-/-}$ mice are significantly increased compared with WT (*Igf1*$^{+/+}$) mice. B, EAT weight in *Igf1*$^{+/-}$ and *Igf1*$^{-/-}$ mice showed no difference compared with WT mice. *, $P < 0.05$. BM, Body mass.

significant increase in thyroid weight. However, a direct transfer of our data to human pathology, especially papillary tumorigenesis, would not be appropriate until we better understand the mechanism that leads to papillary structures and compensates hormone synthesis.

Materials and Methods

Generation of *Igf1r*^{TgCre} mice

Igf1r$^{flox/wt}$ mice (22) were crossed with mice on a mixed (C57BL/6 × 129/Sv) genetic background carrying the mouse *Tg* Cre transgene provided by Professor S. Offermanns (Institut for Pharmacology, University of Heidelberg, Germany) (42).

Mice lacking one or two WT alleles of the *Igf1r* in the thyroid (*Igf1r*$^{+/-}$ or *Igf1r*$^{-/-}$) were derived by crossing male *Igf1r*$^{flox/wt}$ mice with female *Igf1r*$^{flox/wt}$ mice expressing the Cre recombinase under the control of the Tg promoter/enhancer on one allele (Fig. 1A). All mice were housed in pathogen-free facilities in groups of three to five animals at 22 ± 2 C on a 12-h light, 12-h dark cycle. Animals were fed a standard chow diet (Altromin, Lage, Germany) and had also *ad libitum* access to water. Food was withdrawn only if required for an experiment. All experiments were performed in accordance with the rules for animal care of the local government authorities (Landesdirektion Leipzig, Germany) and were approved by the institutional animal care and use committee.

Molecular characterization and genotyping of mice

Genotyping was performed by PCR using genomic DNA isolated from the tail tip. In brief, genomic DNA was prepared by using the DNeasy kit (QIAGEN, Hilden, Germany). The following two primer pairs were used to genotype *Igf1r loxP* sites: 5′-TCC CTC AGG CTT CAT CCG CAA-3′ (forward) and 5′-CTT CAG CTT TGC AGG TGC ACG-3′ (reverse), as well as the *Tg* Cre recombinase 5′-AGT CCC TCA CAT CCT CAG GTT-3′ (forward) and 5′-ATG CCA ACC TCA CAT TTC TTG-3′ (reverse). PCR was performed for 30 cycles (*loxP* sites), 35 cycles (*Tg* Cre) of 95 C, 59 C (*loxP* sites), or 61 C (*Tg* Cre) and 72 C (30 sec each) using the QIAGEN *Taq* Polymerase. DNA from mice with the *Igf1r*^{wt} allele produces a 300-bp band. A 380-bp band is the PCR product of DNA with the *Igf1r*^{flox} allele (Fig. 1B). All mice that were genotyped *Igf1r*$^{flox/flox}$ or *Igf1r*$^{flox/wt}$ and were positive for the *Tg* Cre transgene were considered *Igf1r*$^{-/-}$ or *Igf1r*$^{-/+}$ in the thyroid, respectively. In the following we only refer to the genotypes of the thyroid. For Western blot analysis, tissues were removed and homogenized in homogenization buffer with a mixer mill MM400 (Retsch, Haan, Germany), proteins were isolated using standard techniques, and Western blot analysis was performed with antibodies raised against the IGF-IR β-subunit (C20; Santa Cruz Biotechnology, Inc., Santa Cruz, CA), phospho-AKT (Ser473) (Cell Signaling Technology, Danvers, MA), AKT (pan) (Cell Signaling), p42–44 (Cell Signaling), phosphor p42–44 (Cell Signaling), IGF-IIR/M6PR (Antibodies Online, Aachen, Germany), and β-actin (Sigma, Steinheim, Germany) as loading control.

Phenotypic characterization

Five mice of each genotype [*Igf1r*$^{-/-}$, *Igf1r*$^{+/-}$ or WT (either *Igf1r*$^{wt/wt}$ and *Igf1r*$^{flox/flox}$ without or *Igf1r*$^{wt/wt}$ with the *Tg* Cre transgene)] of both sexes were studied from an age of 1 month up to 1 yr of life. Body weight was recorded weekly. ip glucose GTT and ITT were performed at the age of 3 months. GTT was performed after an overnight fast for 16 h by injecting 2 g/kg body wt glucose and measuring the blood glucose levels after tail vein incision at 0 (baseline), 10, 30, 60, and 120 min after injection. ITT was performed in random-fed animals by injecting 0.75 U/kg body wt human regular insulin (40 U Actrapid; Novo Nordisk, Copenhagen, Denmark). Glucose levels were determined in blood collected from the tail tip immediately before and 15, 30, and 60 min after the ip injection.

Mice were killed at the age of 4 months and 1 yr by an overdose of carbon dioxide. Liver, heart, brain, lung, kidney, spleen, skeletal muscle, sc, brown, and EAT were immediately removed. Serum was collected at 8 wk, 4 months, and 1 yr, respectively, and concentrations of TSH, T_3, and T_4 were measured at the University of Chicago by Dr. R. Weiss (44). ELISA or RIA were used to detect serum levels of insulin (ELISA from DRG, Marburg, Germany), IGF-I, and IGF-II (ELISA and RIA from Mediagnost, Reutlingen, Germany) according to the instructions of the manufacturer.

To examine the function of the thyroid hormone feedback, we studied 6-month-old male and female mice with *Igf1r*$^{+/+}$ and *Igf1r*$^{-/-}$ genotype for their response to exogenous T_3/T_4 treatment as described by Flamant *et al.* (45). Groups of three male and female mice with WT and *Igf1r*$^{-/-}$ genotype were daily injected ip with a mixture of T_4 and T_3 (2.5 mg/kg T_4 and 0.25 mg/kg T_3 in PBS) or vehicle (PBS) for 5 d. Mice were killed and serum was collected as described above.

Animals were placed for 7 d in single cages with running wheels to record their physical activity as turns per day. To test for neurological alterations of the *Igf1r* knockout mice a standardized open field test was performed in which the spontaneous locomotor activities of the mice were manually quantified. For that, mice were placed for 5 min in a dark test area with an area of 1 m (2) and 25 white framed quarters. Every entered field was counted and calculated to the whole entered field number.

cAMP accumulation assays

For cAMP assays 0.7×10^4 HEK cells stably expressing the human TSHR were platted in 96-well plates for 24 h, washed once in serum-free DMEM, followed by a incubation with the same medium containing 1 mM 3-isobutyl-1-methylxanthine (Sigma) in a humidified 5% CO_2 incubator. At the same time, cells were stimulated with appropriate concentrations of bovine TSH and 10 μl of the mice sera for 1 h in 37 C. Reactions were terminated by aspiration of the medium and addition of 150 μl 0.1 N HCl. Supernatants were collected and dried. cAMP content of the cell extracts was determined with a commercial α-screen kit (PerkinElmer, Rodgau, Germany) according to the manufacturer's instructions (46, 47).

In situ hybridization

After the animals were decapitated, brains were removed rapidly, embedded in 2-methylbutane (Sigma) and frozen on dry ice. Sections (20 μm) were cut on a cryostat (Leica, Bentheim, Germany), thaw mounted on silane-treated slides, and stored at

−80 C until further processing. *In situ* hybridization was carried out as described previously (48, 49). Briefly, frozen sections were fixed in a 4% phosphate-buffered paraformaldehyde solution (pH 7.4) for 1 h at room temperature, rinsed with PBS, and treated with 0.4% phosphate-buffered Triton X-100 solution for 10 min. After washing with PBS and water, tissue sections were incubated in 0.1 M triethanolamine (pH 8) containing 0.25% (vol/vol) acetic anhydride for 10 min. After acetylation, sections were rinsed several times with PBS, dehydrated by successive washing with increasing ethanol concentrations, and air dried.

After application of the labeled cRNA probes (final concentration: 5 ng/μl for digoxigenin labeling; 25.000 cpm/μl for ^{35}S labeling), sections were coverslipped and incubated in a humid chamber at 58 C for 16 h. Thereafter, coverslips were removed in 2× saline-sodium citrate (SSC) (0.3 M NaCl; 0.03 M sodium citrate, pH 7.0). The sections were then treated with ribonuclease A (20 μg/ml) and ribonuclease T_1 (1 U/ml) at 37 C for 30 min. Successive washes followed at room temperature in 1×, 0.5×, and 0.2× SSC for 20 min each and in 0.2× SSC at 65 C for 1 h. For digoxigenin-labeled probes, sections were rinsed with P1 (100 mM Tris-HCl; 150 mM NaCl, pH 7.5) and then incubated for 2 h in blocking solution provided by the manufacturer of the kit. After incubation overnight with an anti-digoxigenin antibody conjugated with alkaline phosphatase (1:1000 dilution; Roche, Indianapolis, IN), the tissue sections were washed with P1. Staining proceeded for 2–6 h in substrate solution containing nitroblue tetrazolium (NBT) chloride (340 μg/ml NBT; Biomol, Hamburg, Germany), X-phosphate (175 μg/ml 5-bromo-4-chloro-3-indolyl phosphate; Biomol), 100 mM Tris-HCl, 100 mM NaCl, and 50 mM $MgCl_2$ (pH 9.5). For radioactive probes, the tissue was dehydrated and exposed to Kodak Biomax MR Film (Sigma) for 48 h. For microscopic analysis, the sections were dipped in Kodak NTB2 (Integra Biosciences, Zizers, Switzerland) nuclear emulsion and stored at 4 C. After exposure for 14 d, autoradiograms were developed in Kodak D19 (Sigma) for 4 min and fixed in Kodak Rapid Fix (Sigma) for 4 min. The sections were photographed under dark- or bright-field illumination, and the expression was quantified using the NIH ImageJ software. Sense probes were used to confirm the specificity of the hybridization reaction and did not show any signal.

Immunhistochemistry

Tissue was fixed in 4% buffered formaldehyde and embedded in paraffin. Sections at 0.3 μm were cut with an ultramicrotome (Reichert, Vienna, Austria). Multiple sections were obtained from thyroid and analyzed systematically with respect to follicle size and number. For each genotype, at least five (100× magnifications) per slide were analyzed. Paraffin-embedded sections (3 μm) were dewaxed and rehydrated. Subsequently, sections were pretreated in a microwave oven in 0.1 M citrate buffer (pH 6) for one cycle at 750 W for 3 min and for four cycles of 3 min at 350 W. The LSAB+ System (DAKO Cytomation, Hamburg, Germany) was used for immunodetection. Briefly, slides were incubated with 3% H_2O_2 for 30 min followed by three wash steps with PBS/1% BSA. Unspecific binding was blocked for 30 min, and slides were incubated with monoclonal antibodies against NIS (C-term; Acris Antibodies, San Diego, CA), TG (open biosystems), T_4 (Mybiosource) and TPO (50). Antibodies for cleaved caspase-3 (Asp 175) were obtained from Cell Signaling Technology and used at a concentration of 1:100. Immunoreactivity was demonstrated using a biotinylated secondary antirabbit antibody, streptavidin-conjugated peroxidase, and diamino-benzidine as substrate. Sections were counterstained with hemalaun and mounted in Aquatex (Merck & Co., Inc., Whitehouse Station, NJ).

Quantitative real-time PCR

mRNA expression was measured by quantitative real-time PCR in an ABI PRISM 7000 sequence detector (Applied Biosystems, Darmstadt, Germany) using the TaqMan gene expression assay based on 5′-nuclease chemistry. Total RNA was extracted from organs using TRIzol reagent (Invitrogen GmbH, Karlsruhe, Germany), and 0.5 or 1 μg RNA was reverse transcribed with standard reagents (Life Technologies, Darmstadt, Germany). From each cDNA, 1 μl was amplified in a 10-μl PCR according to manufacturer's instructions (Applied Biosystems). The following TaqMan probe kits were used: *Tg* (Mm00447525_m1), *Igf1r* (*Mm00802831_m1*), *Igf2r* (Mm00439576_m1), *Tshr* (Mm00442027_m1), *Insr* (Mm01211875_m1), *Nis* (Mm00475074_m1), *Tpo* (Mm00456355_m1), and *Trh* (Mm01182425_g1).

BRAF sequencing

To test for genetic alterations that could be the cause of papillary structures in mice with targeted *Igf1r* inactivation, we microdissected eight papillary structures from six male and female mice with both $Igf1r^{+/-}$ and $Igf1r^{-/-}$ genotypes (51). We first prepared total RNA using the miRNeasy FFPE kit from QIAGEN according to the instructions of the manufacturer. We then amplified using RT-PCR (see above) part of the BRAF exon that contained the mouse equivalent of human codon 600 frequently mutated in human papillary thyroid carcinoma (52). Primer sequences were as follows: 5′-TCC AGA CAA CTG TTC AAA CTG-3′ and 5′-ATA TAT TTC TTC ATG AAG ACC-3′. The resulting PCR products were directly sequenced using the BigDye Terminator Kit (Life Technologies) on a 3100 Genetic Analyzer (Life Technologies).

Data analysis and statistics

Data are given as means ± SD. Datasets were analyzed for statistical significance using one-way ANOVA corrected by Bonferroni-Holm and a two-tailed unpaired Student's *t* test using the GraphPad Prism 5.02 (Graph Pad Software Inc., La Jolla, CA). $P < 0.05$ was considered significant.

Acknowledgments

We thank Martina Fügenschuh (Institute of Pathology, University of Leipzig, Leipzig, Germany) for the excellent histological work by embedding and cutting our tissues.

Address all correspondence and requests for reprints to: Knut Krohn, PhD, Interdisciplinary Center for Clinical Research, University of Leipzig, Liebigstrasse 21, 04103 Leipzig. E-mail: krok@med.uni-leipzig.de.

This work was supported by a grant from the Interdisciplinary Center for Clinical Research Leipzig (Projects B26 and Z03),

by grant 107831 from Deutsche Krebshilfe (to K.K.), and by a grant of the Deutsche Forschungsgemeinschaft (FU356/ 3-1).

Disclosure Summary: The authors have nothing to disclose.

References

1. **Dumont JE, Maenhaut C, Pirson I, Baptist M, Roger PP** 1991 Growth factors controlling the thyroid gland. Baillieres Clin Endocrinol Metab 5:727–754
2. **Eggo MC, Bachrach LK, Burrow GN** 1990 Interaction of TSH, insulin and insulin-like growth factors in regulating thyroid growth and function. Growth Factors 2:99–109
3. **Kimura T, Van Keymeulen A, Golstein J, Fusco A, Dumont JE, Roger PP** 2001 Regulation of thyroid cell proliferation by TSH and other factors: a critical evaluation of *in vitro* models. Endocr Rev 22:631–656
4. **Cissewski K, Wolf M, Moses AC** 1992 Characterization of insulin-like growth factor receptors in human thyroid tissue. Receptor 2:145–153
5. **Clément S, Refetoff S, Robaye B, Dumont JE, Schurmans S** 2001 Low TSH requirement and goiter in transgenic mice overexpressing IGF-I and IGF-Ir receptor in the thyroid gland. Endocrinology 142: 5131–5139
6. **Völzke H, Friedrich N, Schipf S, Haring R, Lüdemann J, Nauck M, Dörr M, Brabant G, Wallaschofski H** 2007 Association between serum insulin-like growth factor-I levels and thyroid disorders in a population-based study. J Clin Endocrinol Metab 92:4039–4045
7. **Vella V, Sciacca L, Pandini G, Mineo R, Squatrito S, Vigneri R, Belfiore A** 2001 The IGF system in thyroid cancer: new concepts. Mol Pathol 54:121–124
8. **Ciampolillo A, De Tullio C, Perlino E, Maiorano E** 2007 The IGF-I axis in thyroid carcinoma. Curr Pharm Des 13:729–735
9. **Bruni P, Boccia A, Baldassarre G, Trapasso F, Santoro M, Chiappetta G, Fusco A, Viglietto G** 2000 PTEN expression is reduced in a subset of sporadic thyroid carcinomas: evidence that PTEN-growth suppressing activity in thyroid cancer cells mediated by p27kip1. Oncogene 19:3146–3155
10. **Wang Y, Hou P, Yu H, Wang W, Ji M, Zhao S, Yan S, Sun X, Liu D, Shi B, Zhu G, Condouris S, Xing M** 2007 High prevalence and mutual exclusivity of genetic alterations in the phosphatidylinositol-3-kinase/akt pathway in thyroid tumors. J Clin Endocrinol Metab 92:2387–2390
11. **Dupont J, Holzenberger M** 2003 Biology of insulin-like growth factors in development. Birth Defects Res C Embryo Today 69: 257–271
12. **Butler AA, Yakar S, Gewolb IH, Karas M, Okubo Y, LeRoith D** 1998 Insulin-like growth factor-I receptor signal transduction: at the interface between physiology and cell biology. Comp Biochem Physiol B Biochem Mol Biol 121:19–26
13. **Liu JP, Baker J, Perkins AS, Robertson EJ, Efstratiadis A** 1993 Mice carrying null mutations of the genes encoding insulin-like growth factor I (Igf-1) and type 1 IGF receptor (Igf1r). Cell 75:59–72
14. **Holzenberger M, Dupont J, Ducos B, Leneuve P, Géloën A, Even PC, Cervera P, Le Bouc Y** 2003 IGF-1 receptor regulates lifespan and resistance to oxidative stress in mice. Nature 421:182–187
15. **Kappeler L, De Magalhaes Filho C, Dupont J, Leneuve P, Cervera P, Périn L, Loudes C, Blaise A, Klein R, Epelbaum J, Le Bouc Y, Holzenberger M** 2008 Brain IGF-1 receptors control mammalian growth and lifespan through a neuroendocrine mechanism. PLoS Biol 6:e254
16. **Baker J, Liu JP, Robertson EJ, Efstratiadis A** 1993 Role of insulin-like growth factors in embryonic and postnatal growth. Cell 75: 73–82
17. **Zhang M, Xuan S, Bouxsein ML, von Stechow D, Akeno N, Faugere MC, Malluche H, Zhao G, Rosen CJ, Efstratiadis A, Clemens TL** 2002 Osteoblast-specific knockout of the insulin-like growth factor (IGF) receptor gene reveals an essential role of IGF signaling in bone matrix mineralization. J Biol Chem 277:44005–44012
18. **He J, Rosen CJ, Adams DJ, Kream BE** 2006 Postnatal growth and bone mass in mice with IGF-I haploinsufficiency. Bone 38:826–835
19. **Fernández AM, Dupont J, Farrar RP, Lee S, Stannard B, Le Roith D** 2002 Muscle-specific inactivation of the IGF-I receptor induces compensatory hyperplasia in skeletal muscle. J Clin Invest 109: 347–355
20. **Coleman ME, DeMayo F, Yin KC, Lee HM, Geske R, Montgomery C, Schwartz RJ** 1995 Myogenic vector expression of insulin-like growth factor I stimulates muscle cell differentiation and myofiber hypertrophy in transgenic mice. J Biol Chem 270:12109–12116
21. **Kulkarni RN, Holzenberger M, Shih DQ, Ozcan U, Stoffel M, Magnuson MA, Kahn CR** 2002 β-Cell-specific deletion of the Igf1 receptor leads to hyperinsulinemia and glucose intolerance but does not alter β-cell mass. Nat Genet 31:111–115
22. **Klöting N, Koch L, Wunderlich T, Kern M, Ruschke K, Krone W, Brüning JC, Blüher M** 2008 Autocrine IGF-1 action in adipocytes controls systemic IGF-1 concentrations and growth. Diabetes 57: 2074–2082
23. **Eszlinger M, Krohn K, Beck M, Kipling D, Forbes-Robertson S, Läuter J, Toenjes A, Wynford-Thomas D, Paschke R** 2006 Comparison of differential gene expression of hot and cold thyroid nodules with primary epithelial cell culture models by investigation of co-regulated gene sets. Biochim Biophys Acta 1763:263–271
24. **Kosir R, Acimovic J, Golicnik M, Perse M, Majdic G, Fink M, Rozman D** 2010 Determination of reference genes for circadian studies in different tissues and mouse strains. BMC Mol Biol 11: 60.:60
25. **Hoperia V, Larin A, Jensen K, Bauer A, Vasko V** 2010 Thyroid fine needle aspiration biopsies in children: study of cytological-histological correlation and immunostaining with thyroid peroxidase monoclonal antibodies. Int J Pediatr Endocrinol 2010:690108
26. **Mazumder S, Plesca D, Almasan A** 2008 Caspase-3 activation is a critical determinant of genotoxic stress-induced apoptosis. Methods Mol Biol 414:13–21
27. **Bauer M, Heinz A, Whybrow PC** 2002 Thyroid hormones, serotonin and mood: of synergy and significance in the adult brain. Mol Psychiatry 7:140–156
28. **Samuels MH, Schuff KG, Carlson NE, Carello P, Janowsky JS** 2008 Health status, mood, and cognition in experimentally induced subclinical thyrotoxicosis. J Clin Endocrinol Metab 93:1730–1736
29. **Karl T, Pabst R, von Hörsten S** 2003 Behavioral phenotyping of mice in pharmacological and toxicological research. Exp Toxicol Pathol 55:69–83
30. **Kim CS, Zhu X** 2009 Lessons from mouse models of thyroid cancer. Thyroid 19:1317–1331
31. **Zeiger MA, Saji M, Gusev Y, Westra WH, Takiyama Y, Dooley WC, Kohn LD, Levine MA** 1997 Thyroid-specific expression of cholera toxin A1 subunit causes thyroid hyperplasia and hyperthyroidism in transgenic mice. Endocrinology 138:3133–3140
32. **Fiore E, Rago T, Provenzale MA, Scutari M, Ugolini C, Basolo F, Di Coscio G, Berti P, Grasso L, Elisei R, Pinchera A, Vitti P** 2009 Lower levels of TSH are associated with a lower risk of papillary thyroid cancer in patients with thyroid nodular disease: thyroid autonomy may play a protective role. Endocr Relat Cancer 16: 1251–1260
33. **Nikiforov YE** 2008 Thyroid carcinoma: molecular pathways and therapeutic targets. Mod Pathol 21(Suppl 2):S37–S43
34. **Garcia-Jiménez C, Santisteban P** 2007 TSH signalling and cancer. Arq Bras Endocrinol Metabol 51:654–671
35. **Paschke R, Ludgate M** 1997 The thyrotropin receptor in thyroid diseases. N Engl J Med 337:1675–1681
36. **Boelaert K** 2009 The association between serum TSH concentration and thyroid cancer. Endocr Relat Cancer 16:1065–1072

37. **Arufe MC, Lu M, Lin RY** 2009 Differentiation of murine embryonic stem cells to thyrocytes requires insulin and insulin-like growth factor-1. Biochem Biophys Res Commun 381:264–270
38. **Larsen PR** 1982 Thyroid-pituitary interaction: feedback regulation of thyrotropin secretion by thyroid hormones. N Engl J Med 306: 23–32
39. **Persani L** 1998 Hypothalamic thyrotropin-releasing hormone and thyrotropin biological activity. Thyroid 8:941–946
40. **Zhang H, Fagan DH, Zeng X, Freeman KT, Sachdev D, Yee D** 2010 Inhibition of cancer cell proliferation and metastasis by insulin receptor downregulation. Oncogene 29:2517–2527
41. **Ledent C, Coppee F, Dumont JE, Vassart G, Parmentier M** 1996 Transgenic models for proliferative and hyperfunctional thyroid diseases. Exp Clin Endocrinol Diabetes 104(Suppl 3):43–46
42. **Kero J, Ahmed K, Wettschureck N, Tunaru S, Wintermantel T, Greiner E, Schütz G, Offermanns S** 2007 Thyrocyte-specific Gq/G11 deficiency impairs thyroid function and prevents goiter development. J Clin Invest 117:2399–2407
43. **Moeller LC, Alonso M, Liao X, Broach V, Dumitrescu A, Van Sande J, Montanelli L, Skjei S, Goodwin C, Grasberger H, Refetoff S, Weiss RE** 2007 Pituitary-thyroid setpoint and thyrotropin receptor expression in consomic rats. Endocrinology 148:4727–4733
44. **Weiss RE, Gehin M, Xu J, Sadow PM, O'Malley BW, Chambon P, Refetoff S** 2002 Thyroid function in mice with compound heterozygous and homozygous disruptions of SRC-1 and TIF-2 coactivators: evidence for haploinsufficiency. Endocrinology 143:1554–1557
45. **Flamant F, Poguet AL, Plateroti M, Chassande O, Gauthier K, Streichenberger N, Mansouri A, Samarut J** 2002 Congenital hypothyroid Pax8(−/−) mutant mice can be rescued by inactivating the TRα gene. Mol Endocrinol 16:24–32
46. **Mueller S, Gozu HI, Bircan R, Jaeschke H, Eszlinger M, Luebling-hoff J, Krohn K, Paschke R** 2009 Cases of borderline in vitro constitutive thyrotropin receptor activity: how to decide whether a thyrotropin receptor mutation is constitutively active or not? Thyroid 19:765–773
47. **Mueller S, Kleinau G, Jaeschke H, Paschke R, Krause G** 2008 Extended hormone binding site of the human thyroid stimulating hormone receptor: distinctive acidic residues in the hinge region are involved in bovine thyroid stimulating hormone binding and receptor activation. J Biol Chem 283:18048–18055
48. **Mittag J, Davis B, Vujovic M, Arner A, Vennström B** 2010 Adaptations of the autonomous nervous system controlling heart rate are impaired by a mutant thyroid hormone receptor-α1. Endocrinology 151:2388–2395
49. **Schäfer MK, Day R** 1995 In situ hybridization techniques to study processing enzyme expression at the cellular level. Methods Neurosci 23:16–44
50. **Ruf J, Toubert ME, Czarnocka B, Durand-Gorde JM, Ferrand M, Carayon P** 1989 Relationship between immunological structure and biochemical properties of human thyroid peroxidase. Endocrinology 125:1211–1218
51. **Krohn K, Wohlgemuth S, Gerber H, Paschke R** 2000 Hot microscopic areas of iodine-deficient euthyroid goitres contain constitutively activating TSH receptor mutations. J Pathol 192:37–42
52. **Nikiforov YE** 2011 Molecular analysis of thyroid tumors. Mod Pathol 24(Suppl 2):S34–S43

6. Diskussion

Der Tatsache geschuldet, dass die zwei in dieser Arbeit aufgeführten Publikationen zwar Aspekte der Schilddrüsenphysiologie widerspiegeln, aber dennoch unterschiedliche Fragestellungen zur Grundlage haben, ist diese Diskussion in zwei Abschnitte unterteilt.

6.1 Auswirkungen von Iod auf die Entwicklung einer Schilddrüsenautonomie im Frühstadium

Iod ist ein essentielles Substrat der Hormonsynthese und damit Schlüsselfaktor in der Schilddrüsenphysiologie. Eine gestörte Iod-homöostase wird daher als ein entscheidender Ausgangspunkt in der Schilddrüsenpathologie angesehen. In unserer Studie haben wir ein *in vitro* Modell der Schilddrüsenautonomie hinsichtlich der molekularen Effekte von Iod untersucht und unsere Messungen auf die Funktion, Zellproliferation und globaler Genexpression in genetisch veränderten Thyreozyten fokusiert.

Wir haben Infolge einer erhöhten Iodgabe eine verringerte Genexpressionen in normalen und autonom agierenden FRTL-5 Klonen für solche Gene gefunden, die maßgeblich an der Schilddrüsenfunktion beteiligt sind: *Tpo*, *Nis, Thrsp* und *Iyd*. Eine verminderte Expression funktioneller Gene der Schilddrüse wurde ebenfalls in einer Untersuchung von Leoni et al. mit PCCl-3 Zellen mittels SAGE Analyse bei analogen Iodkonzentrationen beschrieben (63). Diese Beobachtungen gehen ebenfalls mit dem Wolff-Chaikoff-Effekt konform, der die Inhibierung der Schilddrüsenhormonsynthese und dessen Metabolismus durch Iod beschreibt (64;65).

Zudem konnten wir in unseren Experimenten eine Inhibierung des Zellwachstums von FRTL-5 Klonen mit Wildtyp und mutiertem TSHR beobachten. Hierbei zeigte sich der Effekt in den Mutanten und bei TSH Entzug am Stärksten, was dem klinischen Äquivalent der subklinischen oder offenkundigen Hyperthyreose entspräche. Diese Beobachtungen wurden bereits von Al-Kafahji et al. (56) berichtet, die wir nun mit deutlich niedrigeren Iodkonzentrationen (1mM) reproduzieren konnten. In weiterführenden

Untersuchungen konnte dann gezeigt werden, dass die Verminderung des Zellwachstums sehr wahrscheinlich auf eine vermehrte Apoptose und einen Zellzyklus Arrest (Go/ G1 und G2) zurückzuführen ist (66;67). Diese Ergebnisse zeigten nur marginale Unterschiede zwischen den FRTL-5 Klonen mit einem Wildtyp TSHR und konstitutiv aktiviertem TSHR, bei dem an Position 629 das Leucin durch ein Phenylalanin ausgetauscht wurde. Die Gabe von TSH in diesen Experimenten ist sehr wahrscheinlich für die geringen Unterschiede verantwortlich.

Auch wenn unsere in vitro Daten nur ein Modell exemplifizieren, so zeigen sie doch, dass Iod das Wachstum und die Funktion gleicherweise in normalen Thyreozyten und in einer künstlich hervorgerufenen Schilddrüsenautonomie verlangsamt und dadurch eine Erklärung liefern könnte, weshalb die Prävalenz der Schilddrüsenautonomie in Regionen mit ausreichender Iodversorgung wie z.B. Japan am geringsten ist, ungeachtet dem verbreiteten Auftreten von TSHR Mutationen (58;68).

6.2 TSH kompensiert den schilddrüsenspezifischen IGF-I Rezeptor Knockout und führt zu papillären Schilddrüsenhyperplasien

Unsere Studie beschreibt zum ersten Mal die Auswirkungen eines gewebsspezifischen IGF-IR Signalausfalls in der Schilddrüse von Mäusen. Unser Mausmodell verhindert die Expression des *Igf1r* Gens in der Schilddrüse und erlaubt dabei eine normale extrinsische Schilddrüsenstimulation und gibt dadurch entscheidende Hinweise auf die Regulation des Schilddrüsenwachstums. Die Schilddrüsen der IGF-IR defizienten Mäuse zeigen ein normales Gewicht, ebenso unterscheiden sich die Serum T_4 und T_3 Konzentrationen der defizienten Tiere nicht von Wildtyp Mäusen. Allerdings kommt es zu einem enormen Anstieg des Serum TSH in IGF-IR Knockouts der Schilddrüse. Dieser gewaltige Serum TSH Anstieg konnte durch exogene Schilddrüsenhormongabe aufgehoben werden, was auf eine normale Funktion des Feedbacks durch die hypothalamisch-hypophysären Achse hindeutet.

Die Schilddrüsenhistologien aller *Igf1r* Knockout Mäuse passen nicht komplett zu einer latenten humanen Hypothyreose sind dem aber sehr ähnlich. Das Schilddrüsengewicht ist normal und die Histologie zeigt eine große Heterogenität mit dem Fokus auf papilläre Strukturen. Diese papillären Strukturen zeigen sich bei 86% der *Igf1r*$^{-/-}$ Mäusen und sind bereits ab einem Alter von 4 Monaten zu beobachten. Ähnliche Häufigkeiten zeigen sich auch bei den *Igf1r*$^{+/-}$ Mäusen, was deutlich daraufhin weißt, dass diese pathologische Histologie eine Gendosiswirkung des IGF-IR ist und ebenfalls im Zusammenhang mit den erhöhten Serum TSH Werten stehen könnte. Der zu Grunde liegende Mechanismus könnte die Aktivierung des MAPK Signalweges sein, der durch die erhöhten Serum TSH Werte stimuliert wird (69). Eine positive Kopplung zwischen dem TSH/ cAMP und dem MAPK/ ERK Signalweg könnte durch eine Aktivierung der G-Protein Untereinheit βγ resultieren und den PI3K Weg einbinden (28). Allerdings sind die Serum TSH Konzentration in unseren Mäusen so hoch, dass auch das cAMP unabhängige Gq Signal des TSHR stimuliert werden könnte (30). Eine weitere Hypothese für die Entwicklung der papillären Strukturen liefert eine *in vitro* Studie mit embryonalen Stammzellen. Arufe et al. (70) konnte zeigen, dass die Differenzierung der murinen Stammzellen in Thyreozyten IGF-I und IGF-IR abhängig ist. Demzufolge könnte eine aberrante Differenzierung durch das Fehlen des *Igf1r* zu den papillären Strukturen führen. Allerdings erklärt dies nicht das Vorhandensein von normalen und papillären Schilddrüsenformationen in unserem Modell.

Die Daten unseres transgenen Modells passen perfekt zu den Ergebnissen des reversen Mausmodells: Überexpression des IGF-IR in Kombination mit IGF-I in der Schilddrüse (33). Diese Mäuse entwickeln Strumen und zeigen erniedrigtes Serum TSH sowie leicht erhöhte T_4 Werte. Das könnte darauf hindeuten, dass das IGF-IR Signal weniger essentiell für die Schilddrüsenhormonsynthese als für das Aufrechterhalten einer Homöostase und normaler Schilddrüsenmorphogenese ist.

Ein direkter Transfer unserer Daten in die humane Pathologie, vor allem der papillären Tumorigenese, ist solange unangemessen, bis wir die Mechanismen der Entstehung von papillären Strukturen und die

Kompensation der Hormonsynthese in IGF-IR defizienten Mäusen besser verstanden haben.

7. Zusammenfassung der Arbeit

Dissertation zur Erlangung des akademischen Grades Dr. rer. med.

Aspekte der Schilddrüsenphysiologie am Beispiel von Jod, TSHR und IGF-IR

eingereicht von: Kathrin Müller
geboren am 17.11.1982
in Karl-Marx-Stadt

angefertigt an: Universität Leipzig
Klinik für Endokrinologie und Nephrologie

Betreuer:
Prof. Dr. PhD, Dagmar Führer-Sakel

PD Dr. Knut Krohn

Einreichung: Mai 2012

Im Rahmen der vorliegenden Arbeit wurden zentrale Aspekte der Schilddrüsenphysiologie am Beispiel von Iod, TSHR und IGF-IR untersucht.

Der Pathologie der Schilddrüsenautonomie liegen konstitutiv aktivierende Mutationen des TSHR zugrunde. Die Prävalenz der Schilddrüsenautonomie ist in Iod armen Regionen deutlich erhöht. Als Ursache für Mutationen im TSHR wird vermehrter oxidativer Stress unter Iodmangel angenommen (Krohn et al. 2007; Maier et al. 2007). Die genauen molekularen Mechanismen konnten bisher noch nicht hinreichend aufgeklärt werden. In diesem Zusammenhang interessierte uns inwiefern eine ausreichende Iodversorgung die Entwicklung bereits autonomer Zellen beeinflussen kann. Das verwendete *in vitro* Modell der Schilddrüsenautonomie mit konstitutiv aktivierenden Mutationen im TSHR wurde bereits in früheren Arbeiten charakterisiert (Führer et al. 2003). Mit Hilfe von Microarray Untersuchungen und Funktionsanalysen, konnten wir deutliche Genregulationen durch Iod an Hand von normalen und autonomen Thyreozyten erkennen. Besonders auffällig war die differentielle Regulation

von Genen, die z.B. in der Proliferation, dem Zellzyklus und metabolischen Prozessen involviert sind. Wesentlich ist, dass trotz einer konstitutiven Aktivierung des TSHR Iod dennoch die Proliferation und Funktion einer frühzeitigen Schilddrüsenautonomie herabsetzt.

Die physiologische Rolle des IGF-IR in der Schilddrüsenphysiologie *in vivo* wurde noch nicht systematisch erforscht. Um die Rolle des IGF-IR in der Schilddrüse im Hinblick auf deren Entwicklung und Metabolismus näher zu untersuchen, wurde ein Mausmodell generiert bei dem der IGF-IR schilddrüsenspezifisch über eine durch den TG Promoter regulierte Cre Rekombinase (*Igf1r*TgCre) ausgeschaltet wurde. Ziel war es nun zu untersuchen, welche Folgen ein thyreoidaler *Igf1r* Knockout auf die Funktion, Morphologie und Entwicklung der murinen Schilddrüse und metabolischer Parameter hat. Dieser Knockout zeigte in den Mäusen keine Veränderungen des Schilddrüsengewichtes und der Serum T_3 Werte, wobei das Serum T_4 nach 8 Wochen leicht absank, nach 4 Monaten aber wieder Normalwerte zeigte. Allerdings waren die Serum TSH Werte bis zu 9fach erhöht. Die Histologie der *Igf1r*$^{-/-}$ Mäuse zeigten mit einer Rate von 86% papilläre Schilddrüsenhyperplasien sowie eine starke Heterogenität der Follikelstruktur, die auch bei den *Igf1r*$^{-/-}$ Mäuse zu finden war. Die molekulare Kompensation des *Igf1r* Knockouts in der Schilddrüse besonders durch TSH konnte durch unsere Untersuchungen nicht hinreichend geklärt werden. Die Daten aus unseren Ergebnissen und eines reversen Mausmodells (Überexpression des IGF-IR und IGF-I) (Clement et al. 2001) weisen daraufhin, dass das IGF-IR Signal weniger essentiell für die Schilddrüsenhormonsynthese ist als für das Aufrechterhalten einer Homöostase und normaler Schilddrüsenmorphogenese.

8. Literaturverzeichnis

1. **Kimura T, Van Keymeulen A, Golstein J, Fusco A, Dumont JE, Roger PP** 2001 Regulation of thyroid cell proliferation by TSH and other factors: a critical evaluation of in vitro models. Endocr Rev 22(5):631-656.

2. **Carrasco N** 1993 Iodide transport in the thyroid gland. Biochim Biophys Acta 1154(1):65-82.

3. **Magnusson RP, Taurog A, Dorris ML** 1984 Mechanisms of thyroid peroxidase- and lactoperoxidase-catalyzed reactions involving iodide. J Biol Chem 259(22):13783-13790.

4. **Taurog A, Dorris ML, Doerge DR** 1996 Mechanism of simultaneous iodination and coupling catalyzed by thyroid peroxidase. Arch Biochem Biophys 330(1):24-32.

5. **Kaminsky SM, Levy O, Salvador C, Dai G, Carrasco N** 1994 Na(+)-I- symport activity is present in membrane vesicles from thyrotropin-deprived non-I(-)-transporting cultured thyroid cells. Proc Natl Acad Sci U S A 91(9):3789-3793.

6. **Gerard CM, Lefort A, Christophe D et al.** 1989 Control of thyroperoxidase and thyroglobulin transcription by cAMP: evidence for distinct regulatory mechanisms. Mol Endocrinol 3(12):2110-2118.

7. **Pierce KL, Premont RT, Lefkowitz RJ** 2002 Seven-transmembrane receptors. Nat Rev Mol Cell Biol 3(9):639-650.

8. **Shacham S, Topf M, Avisar N et al.** 2001 Modeling the 3D structure of GPCRs from sequence. Med Res Rev 21(5):472-483.

9. **Bockaert J, Pin JP** 1999 Molecular tinkering of G protein-coupled receptors: an evolutionary success. EMBO J 18(7):1723-1729.

10. **van Rhee AM, Jacobson KA** 1996 Molecular Architecture of G Protein-Coupled Receptors. Drug Dev Res 37(1):1-38.

11. **Probst WC, Snyder LA, Schuster DI, Brosius J, Sealfon SC** 1992 Sequence alignment of the G-protein coupled receptor superfamily. DNA Cell Biol 11(1):1-20.

12. **Milgrom E, de Roux N, Ghinea N et al.** 1997 Gonadotrophin and thyrotrophin receptors. Horm Res 48 Suppl 4:33-37.

13. **Wonerow P, Schoneberg T, Schultz G, Gudermann T, Paschke R** 1998 Deletions in the third intracellular loop of the thyrotropin receptor. A new mechanism for constitutive activation. J Biol Chem 273(14):7900-7905.

14. **Allgeier A, Laugwitz KL, Van Sande J, Schultz G, Dumont JE** 1997 Multiple G-protein coupling of the dog thyrotropin receptor. Mol Cell Endocrinol 127(1):81-90.

15. **Laugwitz KL, Allgeier A, Offermanns S et al.** 1996 The human thyrotropin receptor: a heptahelical receptor capable of stimulating members of all four G protein families. Proc Natl Acad Sci U S A 93(1):116-120.

16. **Van Sande J, Raspe E, Perret J et al.** 1990 Thyrotropin activates both the cyclic AMP and the PIP2 cascades in CHO cells expressing the human cDNA of TSH receptor. Mol Cell Endocrinol 74(1):R1-R6.

17. **Van Sande J, Swillens S, Gerard C et al.** 1995 In Chinese hamster ovary K1 cells dog and human thyrotropin receptors activate both the cyclic AMP and the phosphatidylinositol 4,5-bisphosphate cascades in the presence of thyrotropin and the cyclic AMP cascade in its absence. Eur J Biochem 229(2):338-343.

18. **Van Sande J, Parma J, Tonacchera M, Swillens S, Dumont J, Vassart G** 1995 Somatic and germline mutations of the TSH receptor gene in thyroid diseases. J Clin Endocrinol Metab 80(9):2577-2585.

19. **Vassart G, Dumont JE** 1992 The thyrotropin receptor and the regulation of thyrocyte function and growth. Endocr Rev 13(3):596-611.

20. **Dumont JE, Maenhaut C, Pirson I, Baptist M, Roger PP** 1991 Growth factors controlling the thyroid gland. Baillieres Clin Endocrinol Metab 5(4):727-754.

21. **Eggo MC, Bachrach LK, Burrow GN** 1990 Interaction of TSH, insulin and insulin-like growth factors in regulating thyroid growth and function. Growth Factors 2(2-3):99-109.

22. **Williams ED** 1995 Mechanisms and pathogenesis of thyroid cancer in animals and man. Mutat Res 333(1-2):123-129.

23. **LeRoith D, Werner H, Beitner-Johnson D, Roberts CT, Jr.** 1995 Molecular and cellular aspects of the insulin-like growth factor I receptor. Endocr Rev 16(2):143-163.

24. **Proud CG** 1994 Translation. Turned on by insulin. Nature 371(6500):747-748.

25. **Cissewski K, Wolf M, Moses AC** 1992 Characterization of insulin-like growth factor receptors in human thyroid tissue. Receptor 2(3):145-153.

26. **Ullrich A, Gray A, Tam AW et al.** 1986 Insulin-like growth factor I receptor primary structure: comparison with insulin receptor suggests structural determinants that define functional specificity. EMBO J 5(10):2503-2512.

27. **Hsu D, Knudson PE, Zapf A, Rolband GC, Olefsky JM** 1994 NPXY motif in the insulin-like growth factor-I receptor is required for efficient ligand-mediated receptor internalization and biological signaling. Endocrinology 134(2):744-750.

28. **Garcia-Jimenez C, Santisteban P** 2007 TSH signalling and cancer. Arq Bras Endocrinol Metabol 51(5):654-671.

29. **Roger PP, van Staveren WC, Coulonval K, Dumont JE, Maenhaut C** 2010 Signal transduction in the human thyrocyte and its perversion in thyroid tumors. Mol Cell Endocrinol 321(1):3-19.

30. **Paschke R, Ludgate M** 1997 The thyrotropin receptor in thyroid diseases. N Engl J Med 337(23):1675-1681.

31. **Roger PP, Servais P, Dumont JE** 1983 Stimulation by thyrotropin and cyclic AMP of the proliferation of quiescent canine thyroid cells cultured in a defined medium containing insulin. FEBS Lett 157(2):323-329.

32. **Vella V, Sciacca L, Pandini G et al.** 2001 The IGF system in thyroid cancer: new concepts. Mol Pathol 54(3):121-124.

33. **Clement S, Refetoff S, Robaye B, Dumont JE, Schurmans S** 2001 Low TSH requirement and goiter in transgenic mice overexpressing IGF-I and IGF-Ir receptor in the thyroid gland. Endocrinology 142(12):5131-5139.

34. **Volzke H, Friedrich N, Schipf S et al.** 2007 Association between serum insulin-like growth factor-I levels and thyroid disorders in a population-based study. J Clin Endocrinol Metab 92(10):4039-4045.

35. **Ciampolillo A, De Tullio C, Perlino E, Maiorano E** 2007 The IGF-I axis in thyroid carcinoma. Curr Pharm Des 13(7):729-735.

36. **Bruni P, Boccia A, Baldassarre G et al.** 2000 PTEN expression is reduced in a subset of sporadic thyroid carcinomas: evidence that PTEN-growth suppressing activity in thyroid cancer cells mediated by p27kip1. Oncogene 19(28):3146-3155.

37. **Wang Y, Hou P, Yu H et al.** 2007 High prevalence and mutual exclusivity of genetic alterations in the phosphatidylinositol-3-kinase/akt pathway in thyroid tumors. J Clin Endocrinol Metab 92(6):2387-2390.

38. **Takahashi MH, Thomas GA, Williams ED** 1995 Evidence for mutual interdependence of epithelium and stromal lymphoid cells in a subset of papillary carcinomas. Br J Cancer 72(4):813-817.

39. **Liu JP, Baker J, Perkins AS, Robertson EJ, Efstratiadis A** 1993 Mice carrying null mutations of the genes encoding insulin-like growth factor I (Igf-1) and type 1 IGF receptor (Igf1r). Cell 75(1):59-72.

40. **Holzenberger M, Dupont J, Ducos B et al.** 2003 IGF-1 receptor regulates lifespan and resistance to oxidative stress in mice. Nature 421(6919):182-187.

41. **Dupont J, Holzenberger M** 2003 Biology of insulin-like growth factors in development. Birth Defects Res C Embryo Today 69(4):257-271.

42. **Kappeler L, De Magalhaes FC, Dupont J et al.** 2008 Brain IGF-1 receptors control mammalian growth and lifespan through a neuroendocrine mechanism. PLoS Biol 6(10):e254.

43. **Baker J, Liu JP, Robertson EJ, Efstratiadis A** 1993 Role of insulin-like growth factors in embryonic and postnatal growth. Cell 75(1):73-82.

44. **Zhang M, Xuan S, Bouxsein ML et al.** 2002 Osteoblast-specific knockout of the insulin-like growth factor (IGF) receptor gene reveals an essential role of IGF signaling in bone matrix mineralization. J Biol Chem 277(46):44005-44012.

45. **He J, Rosen CJ, Adams DJ, Kream BE** 2006 Postnatal growth and bone mass in mice with IGF-I haploinsufficiency. Bone 38(6):826-835.

46. **Fernandez AM, Dupont J, Farrar RP, Lee S, Stannard B, Le Roith D** 2002 Muscle-specific inactivation of the IGF-I receptor induces compensatory hyperplasia in skeletal muscle. J Clin Invest 109(3):347-355.

47. **Coleman ME, DeMayo F, Yin KC et al.** 1995 Myogenic vector expression of insulin-like growth factor I stimulates muscle cell differentiation and myofiber hypertrophy in transgenic mice. J Biol Chem 270(20):12109-12116.

48. **Kulkarni RN, Holzenberger M, Shih DQ et al.** 2002 beta-cell-specific deletion of the Igf1 receptor leads to hyperinsulinemia and glucose intolerance but does not alter beta-cell mass. Nat Genet 31(1):111-115.

49. **Kloting N, Koch L, Wunderlich T et al.** 2008 Autocrine IGF-1 action in adipocytes controls systemic IGF-1 concentrations and growth. Diabetes 57(8):2074-2082.

50. **Parma J, Duprez L, Van Sande J et al.** 1993 Somatic mutations in the thyrotropin receptor gene cause hyperfunctioning thyroid adenomas. Nature 365(6447):649-651.

51. **Kjelsberg MA, Cotecchia S, Ostrowski J, Caron MG, Lefkowitz RJ** 1992 Constitutive activation of the alpha 1B-adrenergic receptor by all amino acid substitutions at a single site. Evidence for a region which constrains receptor activation. J Biol Chem 267(3):1430-1433.

52. **Corvilain B, Van Sande J, Dumont JE, Vassart G** 2001 Somatic and germline mutations of the TSH receptor and thyroid diseases. Clin Endocrinol (Oxf) 55(2):143-158.

53. **Fuhrer D, Lachmund P, Nebel IT, Paschke R** 2003 The thyrotropin receptor mutation database: update 2003. Thyroid 13(12):1123-1126.

54. **Bauch K** 1998 Epidemiology of functional autonomy. Exp Clin Endocrinol Diabetes 106 Suppl 4:S16-S22.

55. **Fuhrer D, Lewis MD, Alkhafaji F et al.** 2003 Biological activity of activating thyroid-stimulating hormone receptor mutants depends on the cellular context. Endocrinology 144(9):4018-4030.

56. **Al Khafaji F, Wiltshire M, Fuhrer D et al.** 2005 Biological activity of activating thyrotrophin receptor mutants: modulation by iodide. J Mol Endocrinol 34(1):209-220.

57. **Laurberg P, Pedersen KM, Vestergaard H, Sigurdsson G** 1991 High incidence of multinodular toxic goitre in the elderly population in a low iodine intake area vs. high incidence of Graves' disease in the young in a high iodine intake area: comparative surveys of thyrotoxicosis epidemiology in East-Jutland Denmark and Iceland. J Intern Med 229(5):415-420.

58. **Nishihara E, Amino N, Maekawa K et al.** 2009 Prevalence of TSH receptor and Gsalpha mutations in 45 autonomously functioning thyroid nodules in Japan. Endocr J 56(6):791-798.

59. **Aghini-Lombardi F, Antonangeli L, Martino E et al.** 1999 The spectrum of thyroid disorders in an iodine-deficient community: the Pescopagano survey. J Clin Endocrinol Metab 84(2):561-566.

60. **Maier J, van Steeg H, van Oostrom C, Paschke R, Weiss RE, Krohn K** 2007 Iodine deficiency activates antioxidant genes and causes DNA damage in the thyroid gland of rats and mice. Biochim Biophys Acta 1773(6):990-999.

61. **Vitale M, Di Matola T, D'Ascoli F et al.** 2000 Iodide excess induces apoptosis in thyroid cells through a p53-independent mechanism involving oxidative stress. Endocrinology 141(2):598-605.

62. **Krohn K, Maier J, Paschke R** 2007 Mechanisms of disease: hydrogen peroxide, DNA damage and mutagenesis in the development of thyroid tumors. Nat Clin Pract Endocrinol Metab 3(10):713-720.

63. **Leoni SG, Galante PA, Ricarte-Filho JC, Kimura ET** 2008 Differential gene expression analysis of iodide-treated rat thyroid follicular cell line PCCl3. Genomics 91(4):356-366.

64. **Clemens PC, Neumann RS** 1989 The Wolff-Chaikoff effect: hypothyroidism due to iodine application. Arch Dermatol 125(5):705.

65. **Eng PH, Cardona GR, Fang SL et al.** 1999 Escape from the acute Wolff-Chaikoff effect is associated with a decrease in thyroid sodium/iodide symporter messenger ribonucleic acid and protein. Endocrinology 140(8):3404-3410.

66. **Smerdely P, Pitsiavas V, Boyages SC** 1993 Evidence that the inhibitory effects of iodide on thyroid cell proliferation are due to arrest of the cell cycle at G0G1 and G2M phases. Endocrinology 133(6):2881-2888.

67. **Smerdely P, Pitsiavas V, Boyages SC** 1995 The G2M arrest caused by iodide is unrelated to the effects of iodide at adenylate cyclase. Thyroid 5(4):325-330.

68. **Gozu HI, Bircan R, Krohn K et al.** 2006 Similar prevalence of somatic TSH receptor and Gsalpha mutations in toxic thyroid nodules in geographical regions with different iodine supply in Turkey. Eur J Endocrinol 155(4):535-545.

69. **Nikiforov YE** 2008 Thyroid carcinoma: molecular pathways and therapeutic targets. Mod Pathol 21 Suppl 2:S37-S43.

70. **Arufe MC, Lu M, Lin RY** 2009 Differentiation of murine embryonic stem cells to thyrocytes requires insulin and insulin-like growth factor-1. Biochem Biophys Res Commun 381(2):264-270.

Eigenständigkeitserklärung

Erklärung über die eigenständige Abfassung der Arbeit

Hiermit erkläre ich, dass ich die vorliegende Arbeit selbständig und ohne unzulässige Hilfe oder Benutzung anderer als der angegebenen Hilfsmittel angefertigt habe. Ich versichere, dass Dritte von mir weder unmittelbar noch mittelbar geldwerte Leistungen für Arbeiten erhalten haben, die im Zusammenhang mit dem Inhalt der vorgelegten Dissertation stehen, und dass die vorgelegte Arbeit weder im Inland noch im Ausland in gleicher oder ähnlicher Form einer anderen Prüfungsbehörde zum Zweck einer Promotion oder eines anderen Prüfungsverfahrens vorgelegt wurde. Alles aus anderen Quellen und von anderen Personen übernommene Material, das in der Arbeit verwendet wurde oder auf das direkt Bezug genommen wird, wurde als solches kenntlich gemacht. Insbesondere wurden alle Personen genannt, die direkt an der Entstehung der vorliegenden Arbeit beteiligt waren.

Leipzig, den 03.05.2012 .....

Kathrin Müller

Curriculum Vitae

Kathrin Haubold geb. Müller
14467 Potsdam

kathrin@haubold.eu.com

Geburtstagstag:	17. November 1982
Nationalität	deutsch
Geburtsort	Karl-Marx-Stadt (jetzt Chemnitz)

Letzte Positionen:

04/ 2012	**wissenschaftliche Mitarbeiterin, GILUPI Nanomedizin GmbH, Abteilung Klinische Studien, Potsdam**
02/ 2011	**Elternzeit**
2008- 2010	**wissenschaftliche Mitarbeiterin/ Doktorandin in der Arbeitsgruppe von Prof. Dr. Dr. Dagmar Führer, Forschungsabteilung der Klinik und Poliklinik für Endokrinologie und Nephrologie, Medizinische Fakultät der Universität Leipzig**

Ausbildung

2008- 2012	**Promotion Dr. rer. med., Universität Leipzig, Leipzig**
2001- 2007	**Ökotrophologie Studium, Justus-Liebig-Universität, Gießen**
2007	**Master of Science, Ernährungswissenschaften**
2005	**Bachelor of Science, Ökotrophologie**
1993- 2001	**Gymnasium, Georgius-Agricola Gymnasium, Chemnitz**
1989- 1993	**Grundschule, Grundschule am Sonnenberg, Chemnitz**

Studiums bezogene Praktika

2005	**Diabetes- und Ernährungsberatung, Diabetesschulungszentrum, Universitätsklinikum Gießen**
2004	**summer school und Praktika am Institut, nutritional engineering, Ege University, Izmir, Türkei**
2004	**Ernährungsberatung, Deutsche Klinik für Integrative Medizin und Naturheilverfahren, Bad Elster**

Publikationen

Publikationen

Müller, K.*, Weidinger, C.*, Führer, D. (2010). Insulin glargine and insulin have identical effects on proliferation and phosphatidylinositol-3-kinase/Akt signalling in rat thyrocytes and human follicular thyroid cancer cells. Diabetologia 53(5):1001-1003.

Klagge, A., Krause, K., **Müller, K.,** Haag, J., and Führer, D. (2010). High-efficient nonviral transfection of the rat thyroid cell line FRTL-5. Horm.Metab Res. **42:** 897-899.

Müller, K., Krohn, K., Eszlinger, M., Ludgate, M., and Führer, D. (2011) Effect of iodine on early stage thyroid autonomy. Genomics **97(2):**94-100.

Weidinger, C., Krause, K., **Müller, K.,** Klagge, A., Führer, D. (2011). FOXO3 is inhibited by oncogenic PI3K/Akt signaling but can be reactivated by the NSAID sulindac sulfide. J. Clin Endocrinol Metab 96(9):E1361-E1371.

Müller, K.*, Führer,D.*, Mittag, J., Klöting, N., Blüher, M., Weiss, R. E., Many, M. C., Kurt, W. S., and Krohn, K. (2011). TSH Compensates Thyroid-Specific IGF-I Receptor Knockout and Causes Papillary Thyroid Hyperplasia. Mol.Endocrinol. **25:** 1867-1879.

Publizierte Abstracts

<u>Vorträge</u>

Impact of iodine on thyroid cell proliferation
24. Arbeitstagung Experimentelle Schilddrüsenforschung (AESF), Berlin

Impact of iodide on gene regulation in thyroid autonomy: preventive infuenced by iodide?
11th Annual Meeting Young Active Research, 2009, München

Expression and regulation of KCNE2 in human thyroid tumours
54. Symposium der Deutschen Gesellschaft für Endokrinologie (DGE), 2011, Hamburg

TSH compensates thyroid specific IGF-1 receptor knockout and causes papillary thyroid tumours
35th annual meeting European Thyroid Association (Eta), 2011, Krakau

Posterpräsentationen

Preventive modulation of genetically determinated thyroid autonomy by iodine
7. Leipzig Research Festival for Life Sciences, 2008, Leipzig

Preventive modulation genetically determinated thyroid autonomy by iodine
52. Symposium der Deutschen Gesellschaft für Endokrinologie (DGE), 2009, Gießen

TSH compensates thyroid specific IGF-1 receptor knockout at the hormone level
8. Leipzig Research Festival for Life Sciences, 2009, Leipzig

TSH compensates thyroid specific IGF-1 receptor knockout at the hormone level
53. Symposium der Deutschen Gesellschaft für Endokrinologie (DGE), 2010, Leipzig

Insulin glargine (Lantus) and normal insulin have identical effects on proliferation and PI3K/AKT signalling in rat thyrocytes and human follicular thyroid cancer cells
53. Symposium der Deutschen Gesellschaft für Endokrinologie (DGE), 2010, Leipzig

Danksagung

Auf meinem Weg hierher haben mich viele Menschen begleitet und unterstützt, denen ich an dieser Stelle von ganzem Herzen Danken möchte.

An erster Stelle möchte ich Knut Krohn und Dagmar Führer danken, ohne sie wäre diese Arbeit wohl nie zu Stande gekommen. Ihre Geduld und konstruktiven Ideen haben mich sehr vorangetrieben. Besonders danke ich Knut für den Einsatz im Maus-OP, der Klonierungsodyssee und vor allem seiner Hilfsbereitschaft.

Eileen, ich danke dir für 3 tolle Jahre in denen du mir stets bei kleinen und größeren Desastern zur Seite standest oder einfach nur zugehört hast. Unserer Klonierungsqueen Steffi danke ich für die zahlreichen Wiederholungen, wenn es bei mir mal wieder nicht funktioniert hat.

Kerstin und Carli danke ich für ihre guten Ideen, den Gesprächen von Bildschirm zu Bildschirm und ihre stetige Bereitschaft mich zu unterstützen.

Liebe Beate, liebe Moni ihr habt mich bei so vielen praktischen Anwendungen unterstütz: Danke!

Nora und Matthias aus der AG Blüher danke ich für ihre geduldige und sanfte Art mich in die Kunst der Mausexperimente einzuführen.

Dem gesamten Endo-Labor danke ich für die tolle Arbeitsatmosphäre und den gelegentlichen Kaffee- und Kickerpausen.

Meinen größten Dank möchte ich allerdings meiner Familie aussprechen, die mich immer wieder motiviert und in meinem Wirken bestätigt hat. Florian, du hast die 3 Jahre trotz vieler Kilometer Entfernung immer zu mir gestanden und mich auf vielen Wegen unterstützt. Michi und Steffi, ihr habt mir die Zeit in Leipzig versüßt und ich hoffe ein Platz auf eurer Couch bleibt mir immer erhalten.

Nachweis über den Anteil von Kathrin Müller an der ausgewählten Publikation

Hiermit erklären wir, dass Frau Kathrin Müller an der Publikation ***TSH compensates thyroid specific IGF-1 receptor knockout and causes papillary thyroid hyperplasia*** in der Zeitschrift ***Molecular Endocrinology*** wesentlichen Anteil trägt, der eine geteilte Erstautorenschaft rechtfertigt. Sie war substanziell an der Konzeption der Arbeit beteiligt und hat die Experimente durchgeführt, die Daten ausgewertet und für die Publikation vorbereitet. Außerdem war Frau Müller maßgeblich an der Interpretation der Ergebnisse beteiligt. Die von Frau Prof. Dr. Dr. Führer erbrachte Leistung beinhaltete ebenfalls eine substanzielle Mitwirkung an der Konzeption der Arbeit und wesentliche Beiträge zum intellektuellen Inhalt der Publikation und zur Revision der Publikation vor der Veröffentlichung.

The authors declare that Kathrin Müller made a significant contribution to the article "***TSH compensates thyroid specific IGF-1 receptor knockout and causes papillary thyroid hyperplasia"*** published in ***Molecular Endocrinology*** that justifies shared first authorship. She and Dr. Führer substantially contributed to the conception, design, execution, analysis and interpretation of data and participated in the writing and revision of the manuscript.

K. [signature]

Kathrin Müller, Klinik für Endokrinologie und Nephrologie, Universität Leipzig

[signature]

Prof. Dr. Dr. Dagmar Führer, Klinik für Endokrinologie und Nephrologie, Universität Leipzig

Jens Mittag [signature]

PhD Jens Mittag, Department of Cell and Molecular Biology, Karolinska Institute

N. Klöting [signature]

Dr. Nora Klöting, Klinik für Endokrinologie und Nephrologie, Universität Leipzig

[signature]

Prof. Dr. Matthias Blüher, Klinik für Endokrinologie und Nephrologie, Universität Leipzig

Prof. Dr. Roy E. Weiss, Section of Adult and Pediatric Endocrinology, Diabetes and Metabolism, University of Chicago,

Prof. Dr. Marie-Christine Many, Universite Catholique de Louvain Medical School, Brüssel

Prof. Dr. Kurt Werner Schmid, Institut für Pathotologie und Neuropathologie, Universität Duisburg-Essen

PD Dr. Knut Krohn, Interdisziplinäres Zentrum für Klinische Forschung, Universität Leipzig